

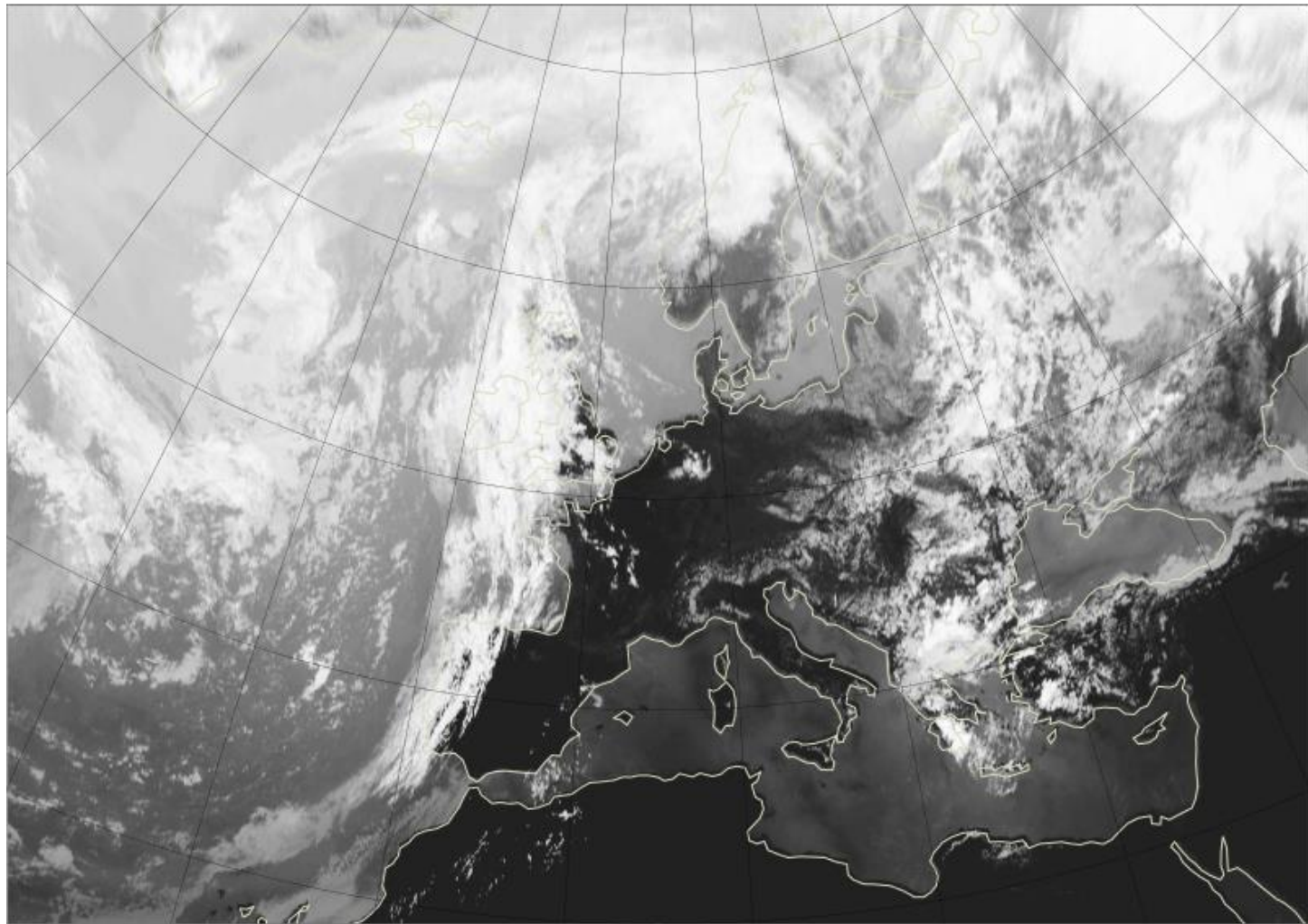
Diagnostics used in the university research context

Christian M. Grams, M. Sprenger, and H. Wernli

with contributions from the entire Atmospheric Dynamics Group, ETH Zurich

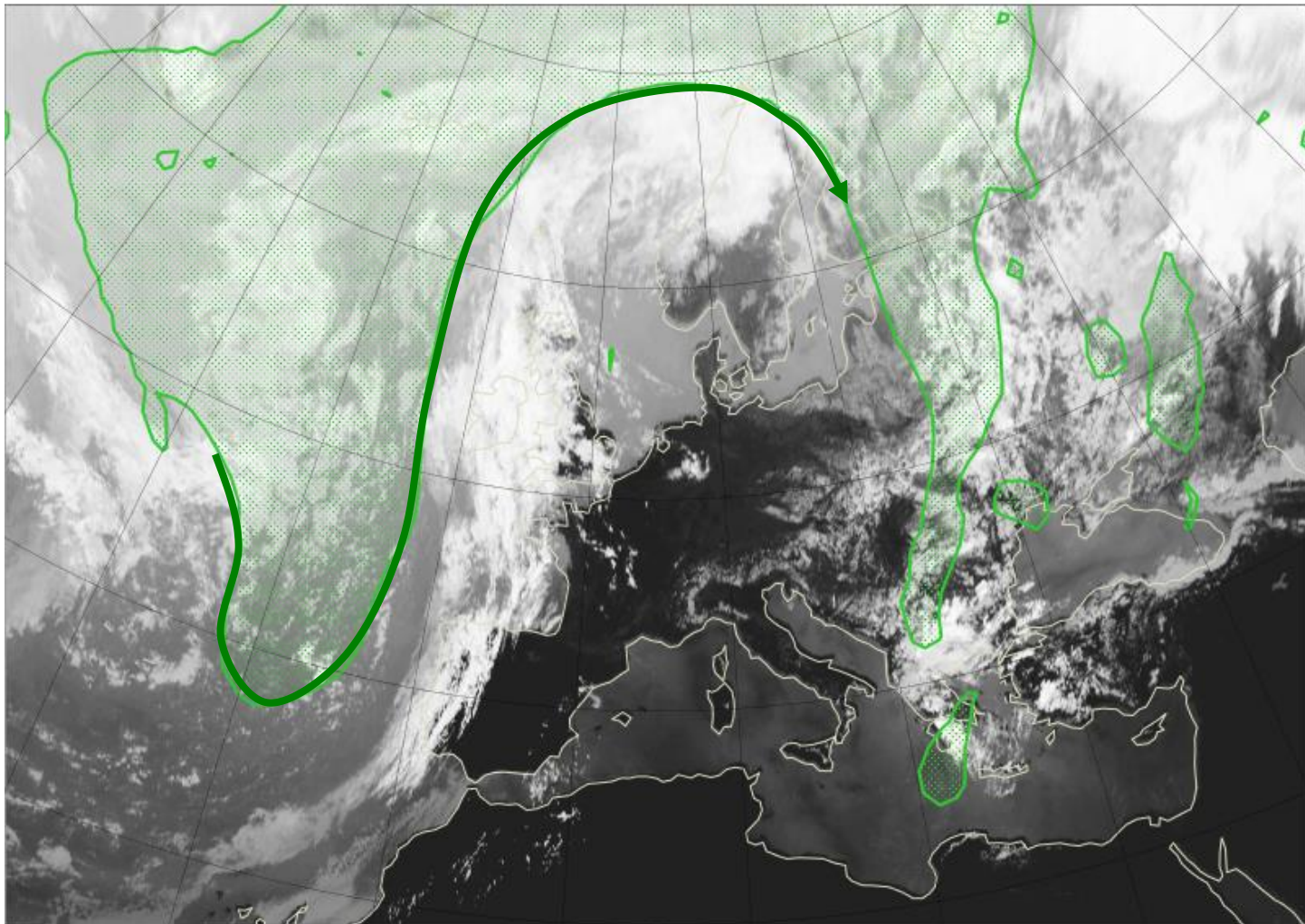


Heatwave Europe July 2015



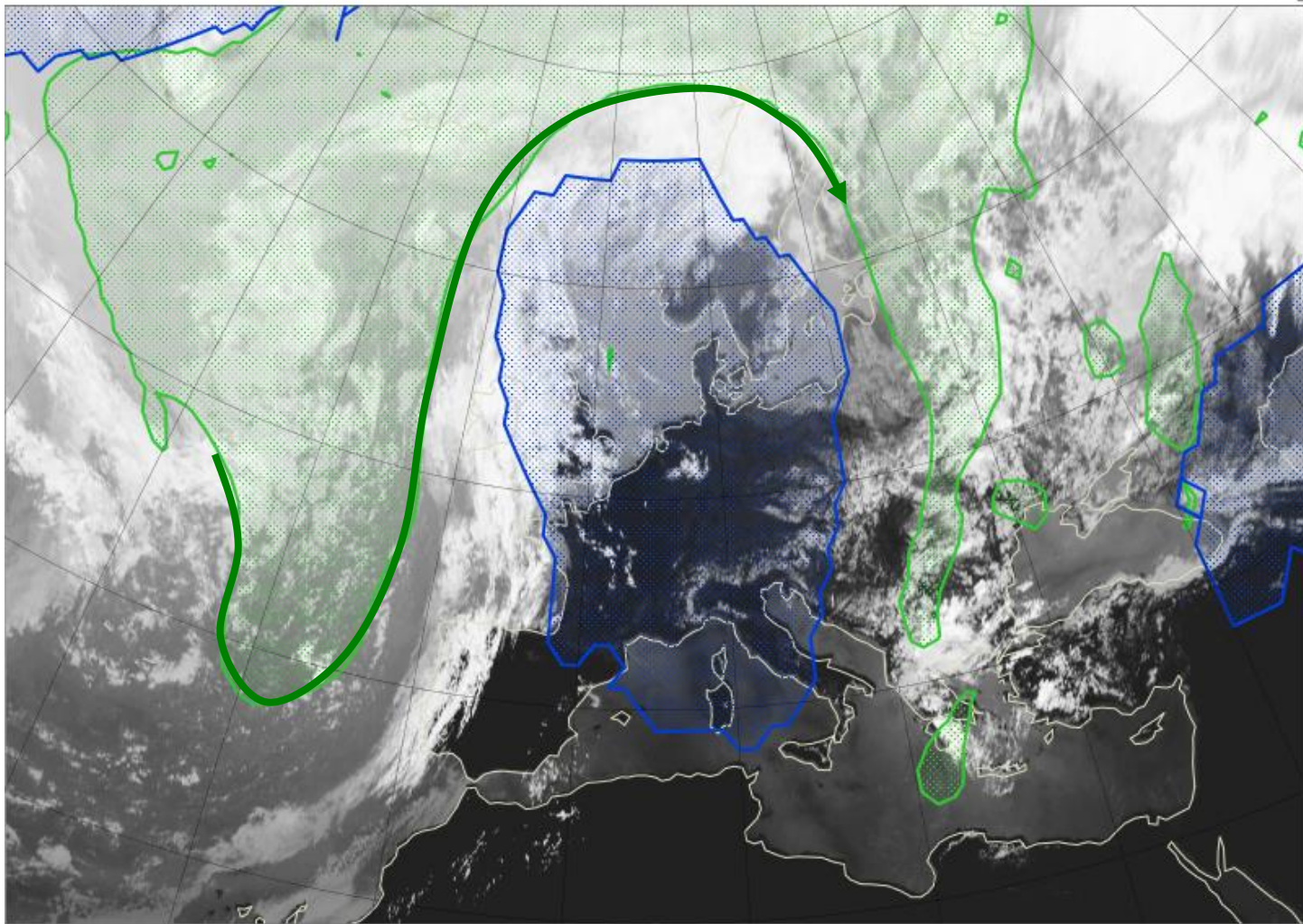
MSG IR satellite 12 UTC 1 July 2015

Heatwave Europe July 2015



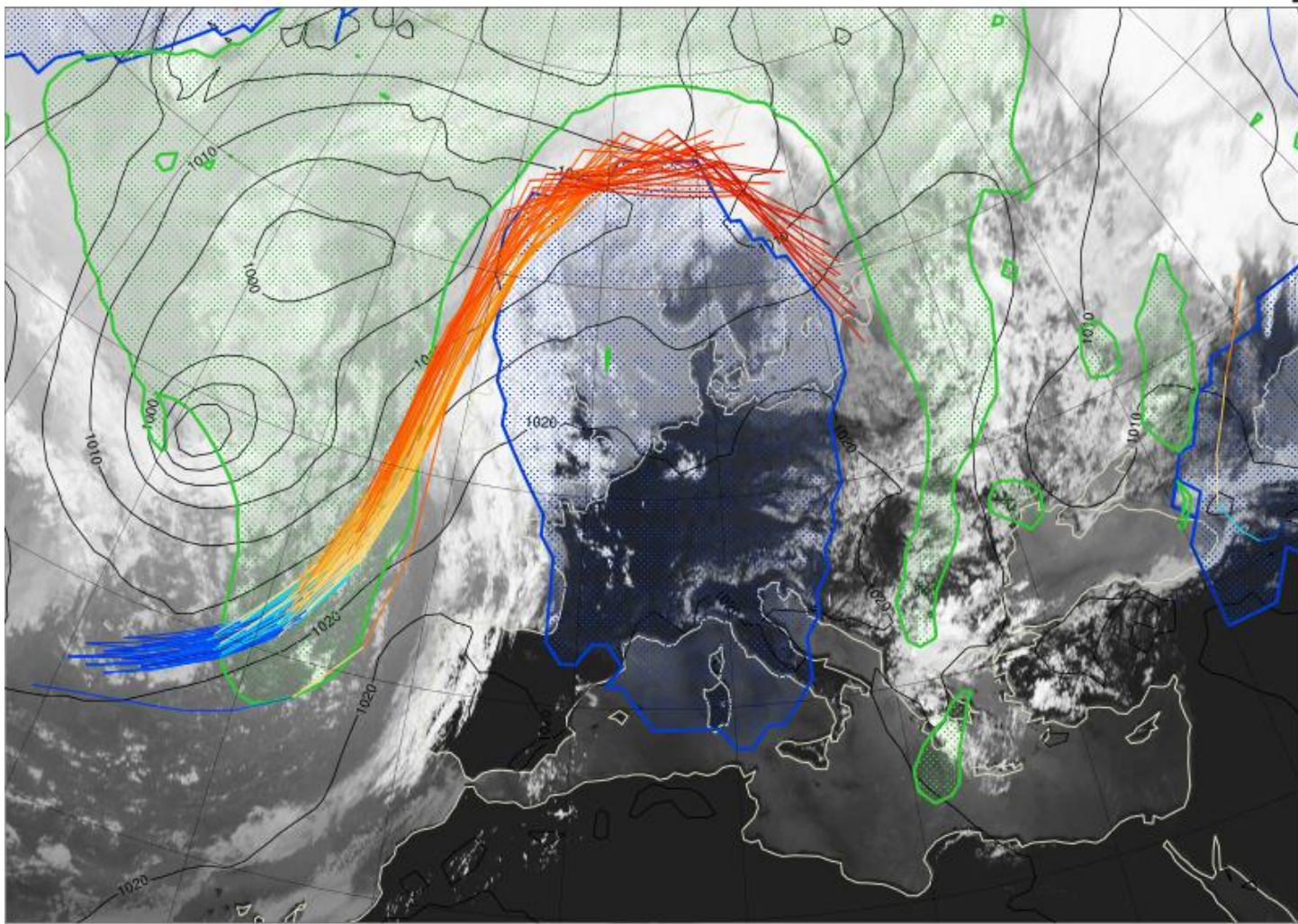
MSG IR satellite 12 UTC 1 July 2015
Jetstream deflected towards Scandinavia (2PVU@325K)

Heatwave Europe July 2015



MSG IR satellite 12 UTC 1 July 2015, jetstream (2PVU@325K)
Atmospheric blocking extends over heat wave region

Heatwave Europe July 2015



MSG IR satellite 12 UTC 1 July 2015, jetstream (2PVU@325K), blocking
Strongly ascending and precipitating airstream – associated with North Atlantic cyclone - reaches into blocking region (MSLP 12 UTC 29 June 2015)

Outline

1. Feature-based diagnostics
2. Diabatic influences on blocking
3. Operational applications
4. A recent forecast bust
5. Demonstration NAWDEX
6. Summary

1. Feature-based diagnostics: Overview

Sprenger, M., G. Fragkoulidis, et al.: Global climatologies of Eulerian and Lagrangian flow features based on ERA-Interim reanalyses. *Bull. Amer. Meteor. Soc.* [doi:10.1175/BAMS-D-15-00299.1](https://doi.org/10.1175/BAMS-D-15-00299.1), in press.

Feature-based diagnostics: Overview

Eulerian	Lagrangian
Cyclones	<i>Warm conveyor belts</i>
Blocking	Strat.-Trop. Exchange
PV streamer	Tropical moisture exports
PV cutoff	<i>Dry intrusions</i> (S. Raveh-Rubin)
Fronts	Cold air outbreaks (L. Papritz, UBergen)
Jetstreams	
Tropopause folds	
Atmospheric rivers (H.Wernli)	
Baroclinicity (L. Papritz, UBergen)	

explained in this talk

monthly clim. freely available

work in progress

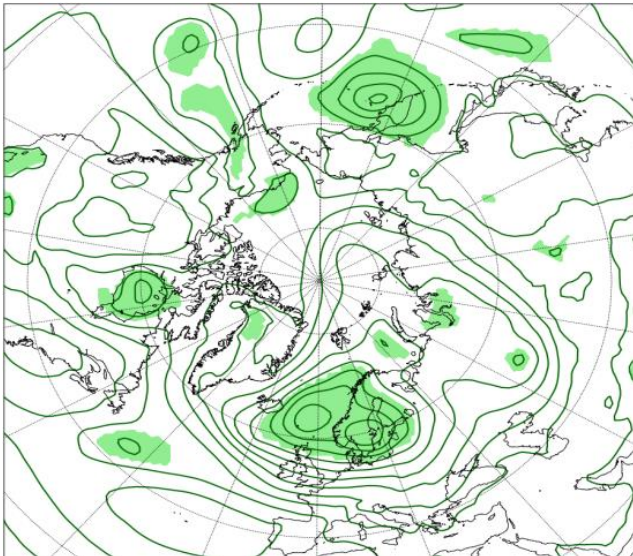
Sprenger, M., G. Frakouidis, et al.: Global climatologies of Eulerian and Lagrangian flow features based on ERA-Interim reanalyses. *Bull. Amer. Meteor. Soc.* [doi:10.1175/BAMS-D-15-00299.1](https://doi.org/10.1175/BAMS-D-15-00299.1), in press.

1. Feature-based diagnostics: cyclones

Sprenger, M., G. Fragkoulidis, et al.: Global climatologies of Eulerian and Lagrangian flow features based on ERA-Interim reanalyses. *Bull. Amer. Meteor. Soc.* [doi:10.1175/BAMS-D-15-00299.1](https://doi.org/10.1175/BAMS-D-15-00299.1), in press.

Wernli, H. and C. Schwierz, 2006: Surface cyclones in the ERA-40 Dataset (1958-2001). Part I: Novel identification method and global climatology. *J. Atmos. Sci.*, **63**, 2486-2507. [doi:10.1175/JAS3766.1](https://doi.org/10.1175/JAS3766.1)

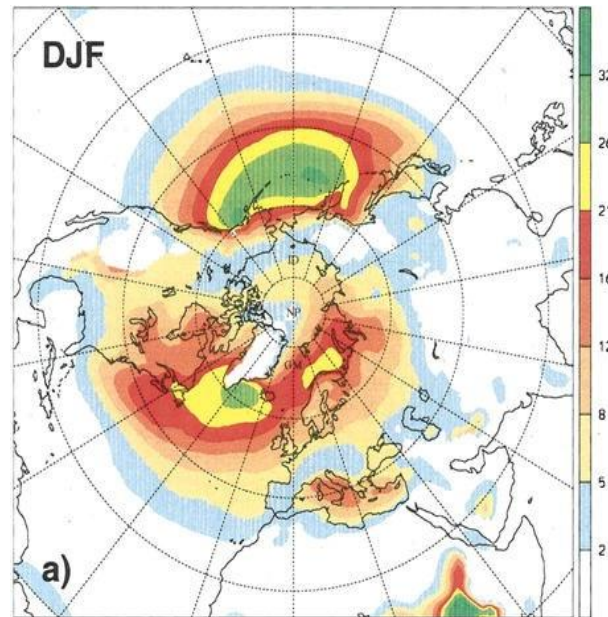
Cyclones



SLP, 00 UTC 27 Feb 1990

- closed SLP contours around minima
- Set 0/1 mask
- unique label for each cyclone
- ranking into 1st, 2nd,... minimum
- Split multi-centre cyclones
- Tracking every 6h

Cyclone frequency DJF



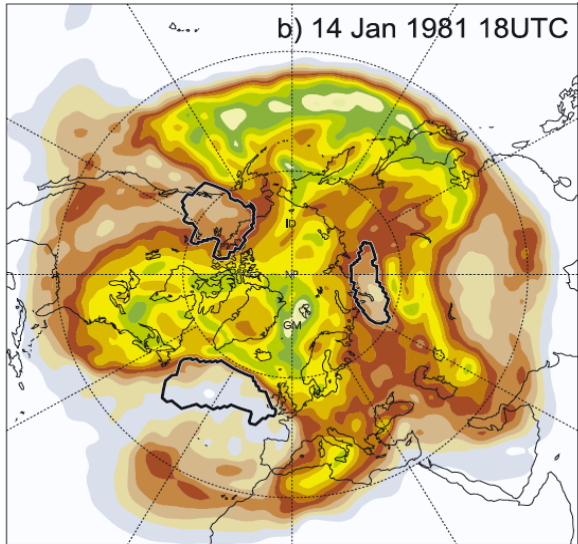
Sprenger, M., G. Fragkoulidis, et al. (2017), *BAMS*, [doi:10.1175/BAMS-D-15-00299.1](https://doi.org/10.1175/BAMS-D-15-00299.1)
Wernli, H. and C. Schwierz, (2006), *JAS*, [doi:10.1175/JAS3766.1](https://doi.org/10.1175/JAS3766.1).

1. Feature-based diagnostics: Blocking

Sprenger, M., G. Fragkoulidis, et al.: Global climatologies of Eulerian and Lagrangian flow features based on ERA-Interim reanalyses. *Bull. Amer. Meteor. Soc.* [doi:10.1175/BAMS-D-15-00299.1](https://doi.org/10.1175/BAMS-D-15-00299.1), in press.

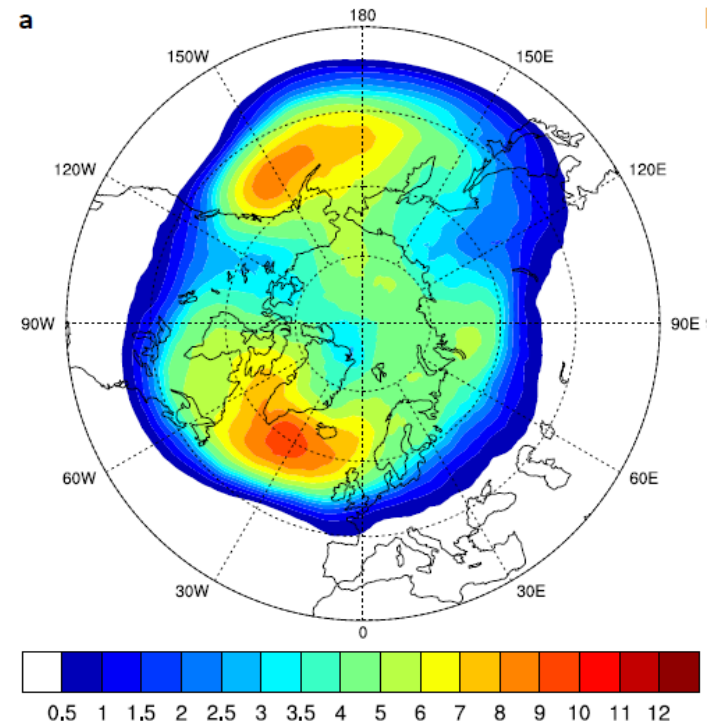
Schwierz, C., M. Croci-Maspoli, and H. C. Davies (2004), Perspicacious indicators of atmospheric blocking, *Geophys. Res. Lett.*, **31**, L06125, [doi:10.1029/2003GL019341](https://doi.org/10.1029/2003GL019341).

Blocking



- calculate **vertically averaged PV** (VAPV) between 500 and 150 hPa
- **negative VAPV anomalies** wrt. monthly climatology < 1.3 PVU
- track anomalies in time
- anomalies living longer than **5 days** (with at least 70% overlap at each 6-hourly time step) are identified as **blocks**

Blocking frequency full year



Sprenger, M., G. Fragkouidis, et al. (2017), *BAMS*, doi:[10.1175/BAMS-D-15-00299.1](https://doi.org/10.1175/BAMS-D-15-00299.1)
Schwierz et al., (2004), *GRL*, doi:[10.1029/2003GL019341](https://doi.org/10.1029/2003GL019341).

1. Feature-based diagnostics: LAGRANTO

Sprenger, M. and Wernli, H. (2015): The LAGRANTO Lagrangian analysis tool - version 2.0, Geosci. Model Dev., 8, 2569–2586, [doi:10.5194/gmd-8-2569-2015](https://doi.org/10.5194/gmd-8-2569-2015).

LAGRANTO

The Lagrangian Analysis Tool

Contact

LAGRANTO:

Heini Wernli

Michael Sprenger

LAGRANTO.OCEAN:

Sebastian Schemm

About

Lagrangian parcel trajectories are widely used in the atmospheric and oceanic sciences, for instance, to identify flow structures in extratropical cyclones (e.g., warm conveyor belts) or ocean eddies, long-range transport pathways of moisture, or to study the physical processes underlying the formation of sea surface temperature, salinity or potential vorticity anomalies.

1. LAGRANTO.ECMWF

It is used to compute air-parcel trajectories typically based on 6-hourly ERA-Interim data on a regular lat/lon grid. In addition it was applied also to 20CR data.

Citation:

Sprenger, M. and Wernli, H. (2015): The LAGRANTO Lagrangian analysis tool - version 2.0, *Geosci. Model Dev.*, **8**, 2569–2586, doi:10.5194/gmd-8-2569-2015.

... [View citation details](#) ...

2. LAGRANTO.COSMO

Is the version used to compute air-parcel trajectories based on the output of the COSMO model. An online and offline version of the tools is available. For the online computation the actual model time step is used, which increase the accuracy of the trajectories.

Citation:

Miltenberger, A.K., Pfahl S., and Wernli H. (2013): An online trajectory module (version 1.0) for the nonhydrostatic

3. LAGRANTO.OCEAN

The ocean version is the latest member of the LAGRANTO family. It can be used to compute ocean-parcel trajectories based on ECMWF's Ocean Reanalysis data (ORAS5). The triangular grid of the input data is transformed and rotated into a regular lat/lon grid. At the boundaries no-normal and no-slip boundary conditions are applied. This version is under development.

Citation:

- Computation of Lagrangian parcel forward/backward trajectories
- Multiple options for selection of subsets (spatial & temporal criteria, physical properties)
- Freely available (versions for IFS, COSMO, WRF, UM)

Sprenger, M. and Wernli, H. (2015): The LAGRANTO Lagrangian analysis tool - version 2.0, *Geosci. Model Dev.*, **8**, 2569–2586, doi:10.5194/gmd-8-2569-2015.

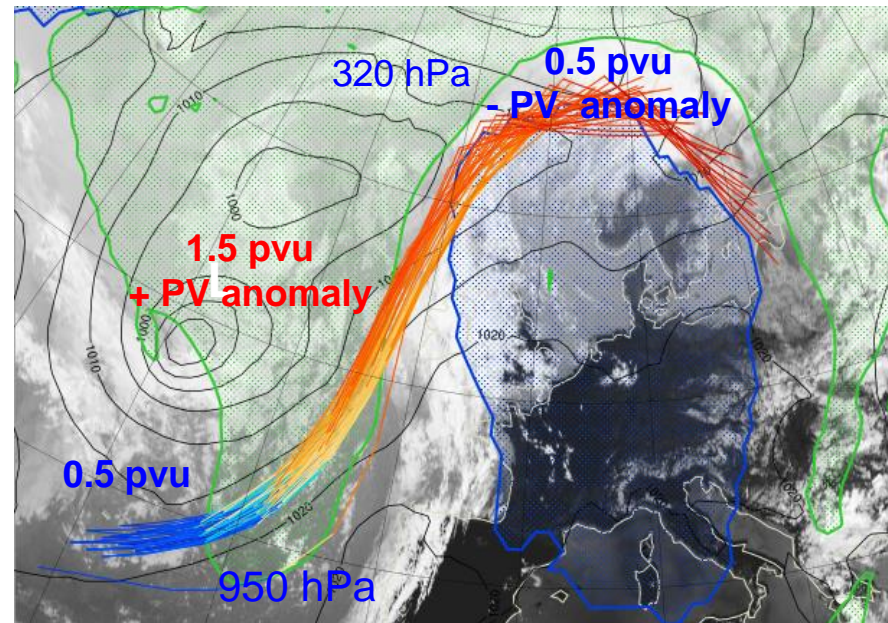
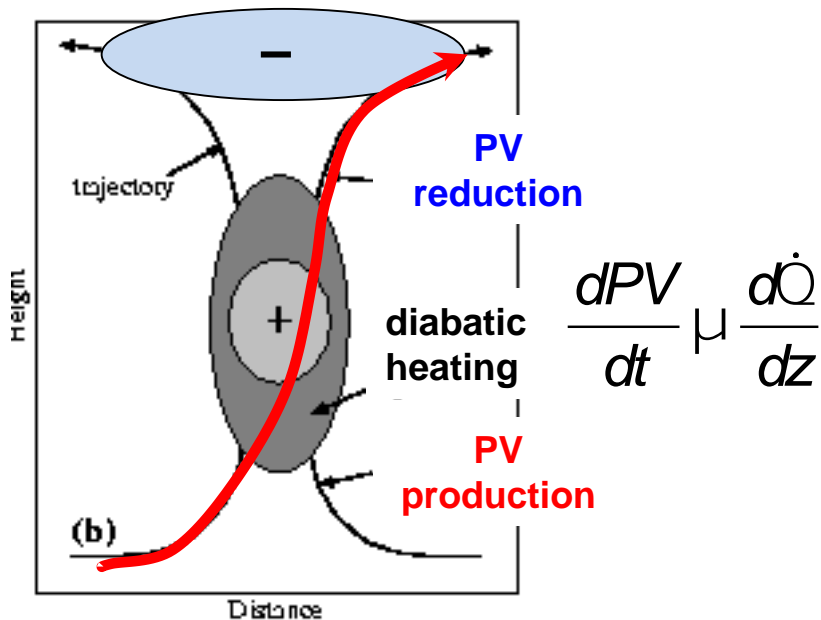
1. Feature-based diagnostics: WCBs

Madonna, E., et al., 2014: Warm Conveyor Belts in the ERA-Interim Dataset (1979–2010). Part I: Climatology and Potential Vorticity Evolution. *J. Climate*, **27**, 3–26, [doi:10.1175/JCLI-D-12-00720.1](https://doi.org/10.1175/JCLI-D-12-00720.1).

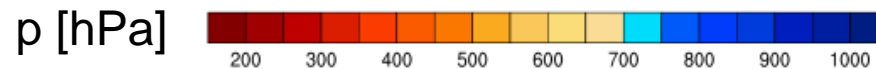
Warm conveyor belts

- rapidly ascending cross isentropic air flows (>600hPa/48h)
- diabatic heating of about 20K / 48h
- diabatic PV **production** below level of maximum heating
- diabatic PV **reduction** and low PV values at upper levels

see WCB clim. by Madonna et al. (2014)

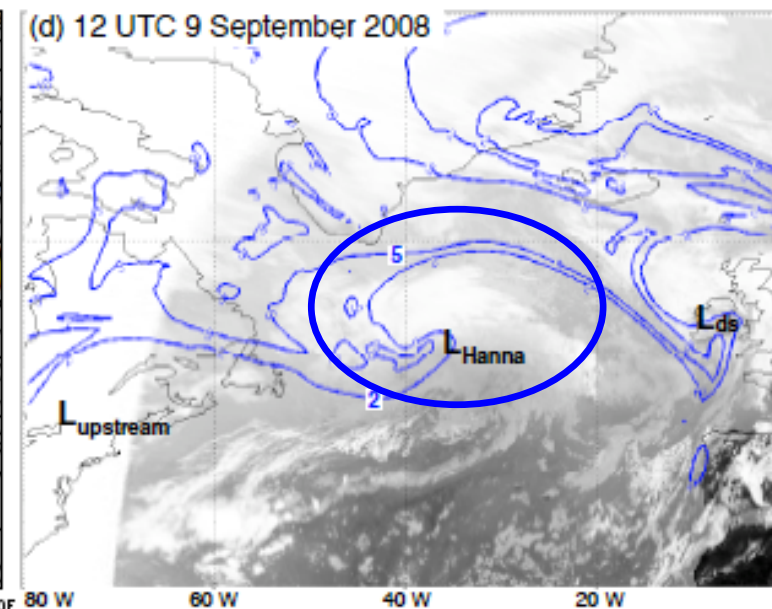
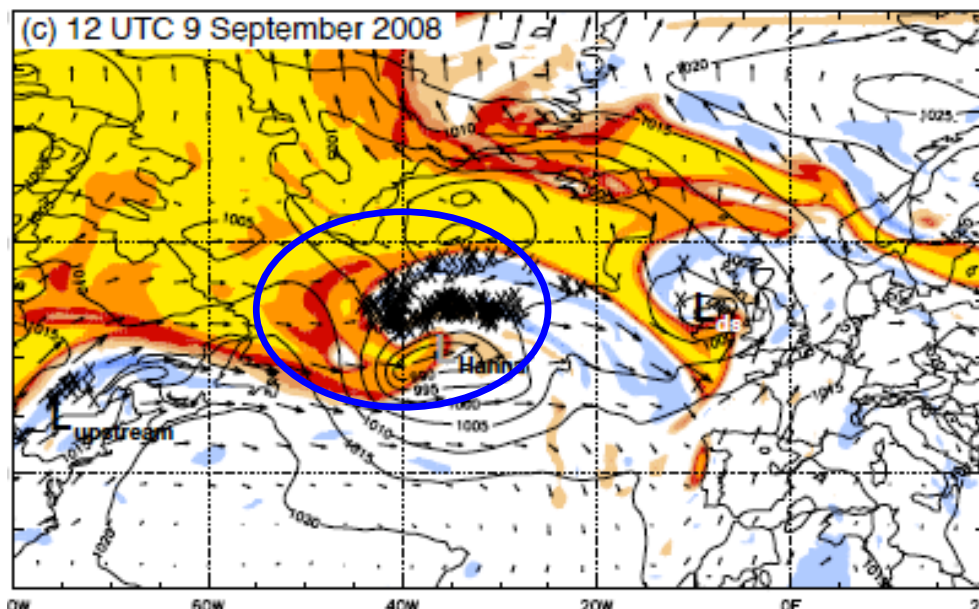


Wernli and Davies (1997), QJRMS



WCB outflow and upper-level flow

PV on 320 K



Grams et al. (2011), QJRMS

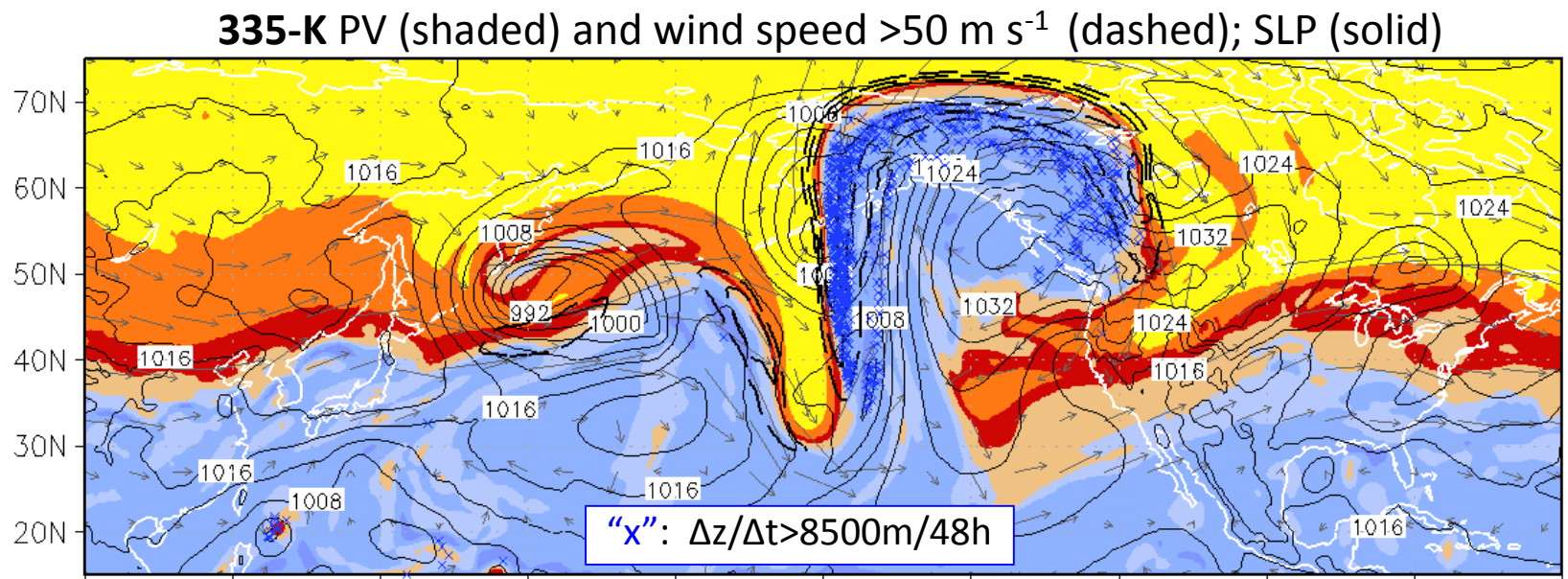
$$\frac{dPV}{dt} = \frac{1}{\rho} \vec{\eta} \cdot \nabla \dot{\Theta} + \frac{1}{\rho} (\nabla \times \vec{F}) \cdot \nabla \Theta$$

Total change
in PV

diabatic PV
modification

frictional
processes

WCB outflow and upper-level flow



Grams and Archambault (2016), MWR, doi: 10.1175/MWR-D-15-0419.1

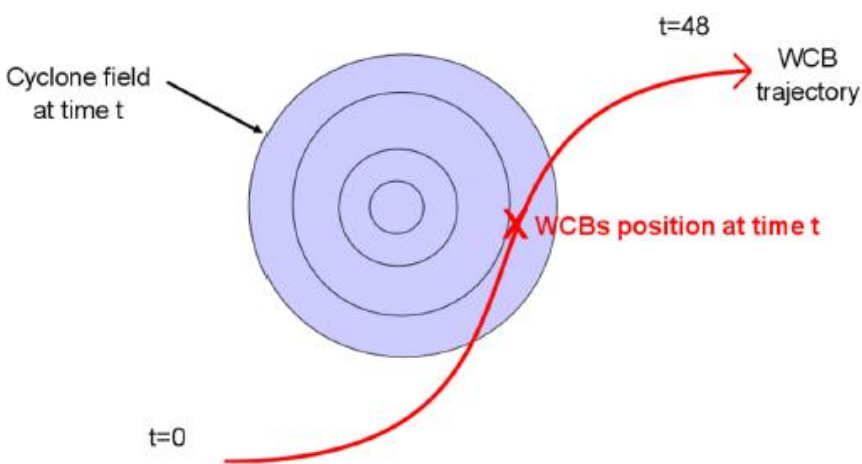


$$\frac{dPV}{dt} = \frac{1}{\rho} \vec{\eta} \cdot \nabla \dot{\Theta} + \frac{1}{\rho} (\nabla \times \vec{F}) \cdot \nabla \Theta$$

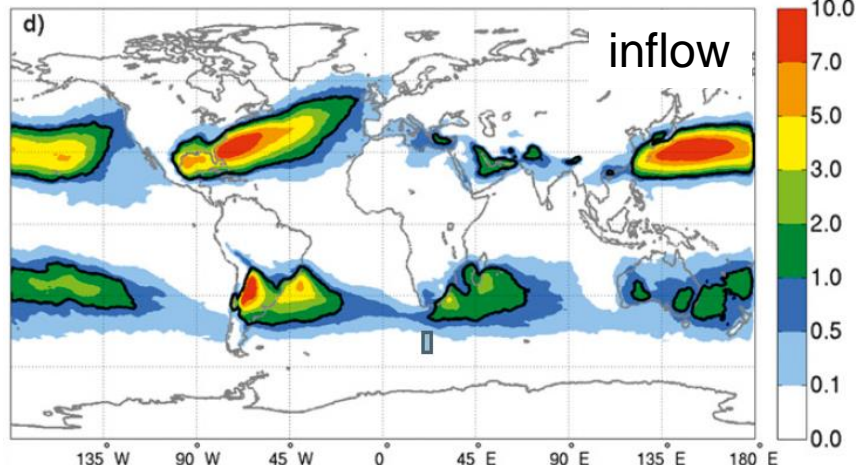
Total change in PV diabatic PV modification frictional processes

WCB climatology

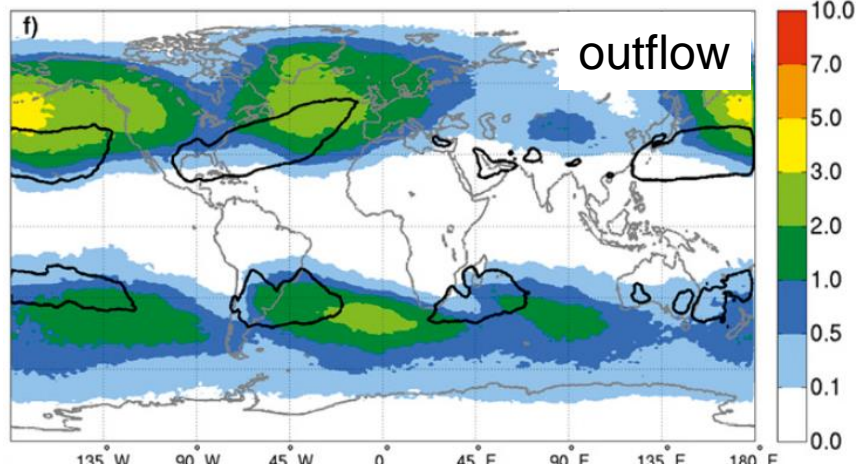
- Ascending more than 600 hPa in 48 h
- vicinity of extratropical cyclone (to exclude rapid ascent in convective systems)
- tracing forward and backward along WCB trajectory: Q, LWC, IWC, RH, TH, PV



WCB frequency DJF



inflow

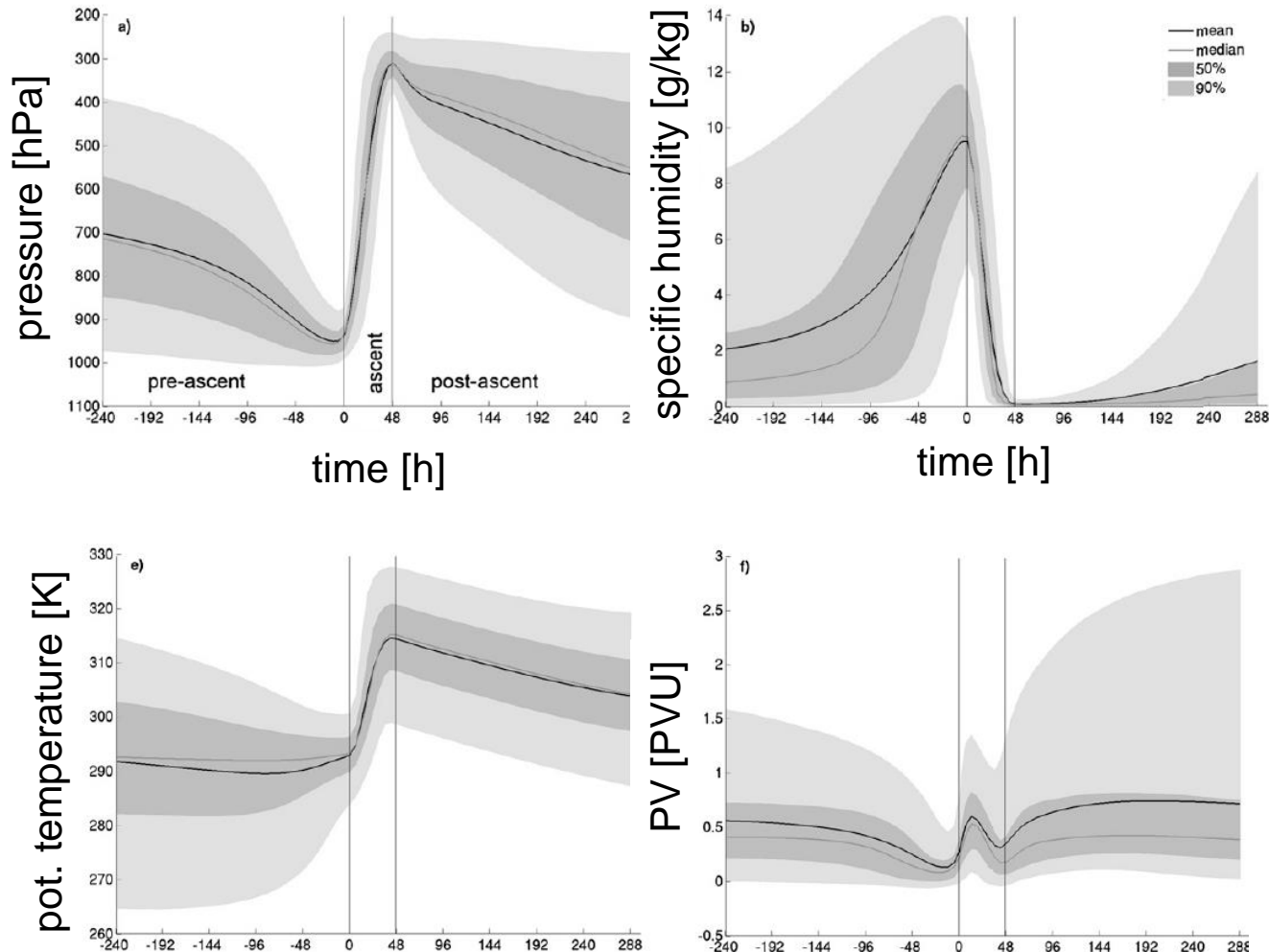


outflow

Madonna, E., et al., 2014: Warm Conveyor Belts in the ERA-Interim Dataset (1979–2010). Part I: Climatology and Potential Vorticity Evolution. *J. Climate*, **27**, 3–26, doi:10.1175/JCLI-D-12-00720.1.

WCB climatology

- Loss of specific humidity (precipitation)
- Cross-isentropic ascent (latent heat release due to condensation)
- Net transport of low-PV air to upper troposphere



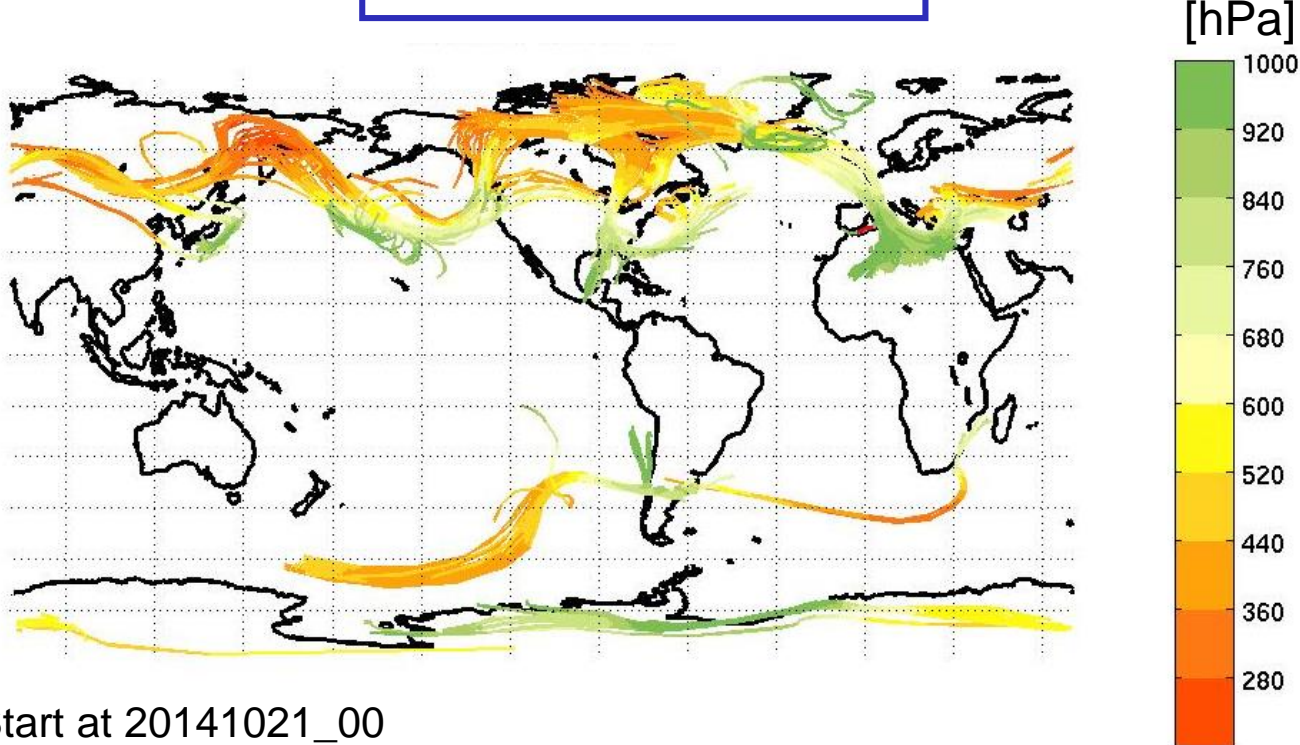
Madonna, E., et al., 2014: Warm Conveyor Belts in the ERA-Interim Dataset (1979–2010). Part I: Climatology and Potential Vorticity Evolution. *J. Climate*, **27**, 3–26, doi:10.1175/JCLI-D-12-00720.1.

1. Feature-based diagnostics: Dry intrusions

Raveh-Rubin, S., 2017: Dry intrusions: Lagrangian climatology and dynamical impact on the planetary boundary layer. *J. Climate*, [doi: 10.1175/JCLI-D-16-0782.1](https://doi.org/10.1175/JCLI-D-16-0782.1)

Dry intrusions

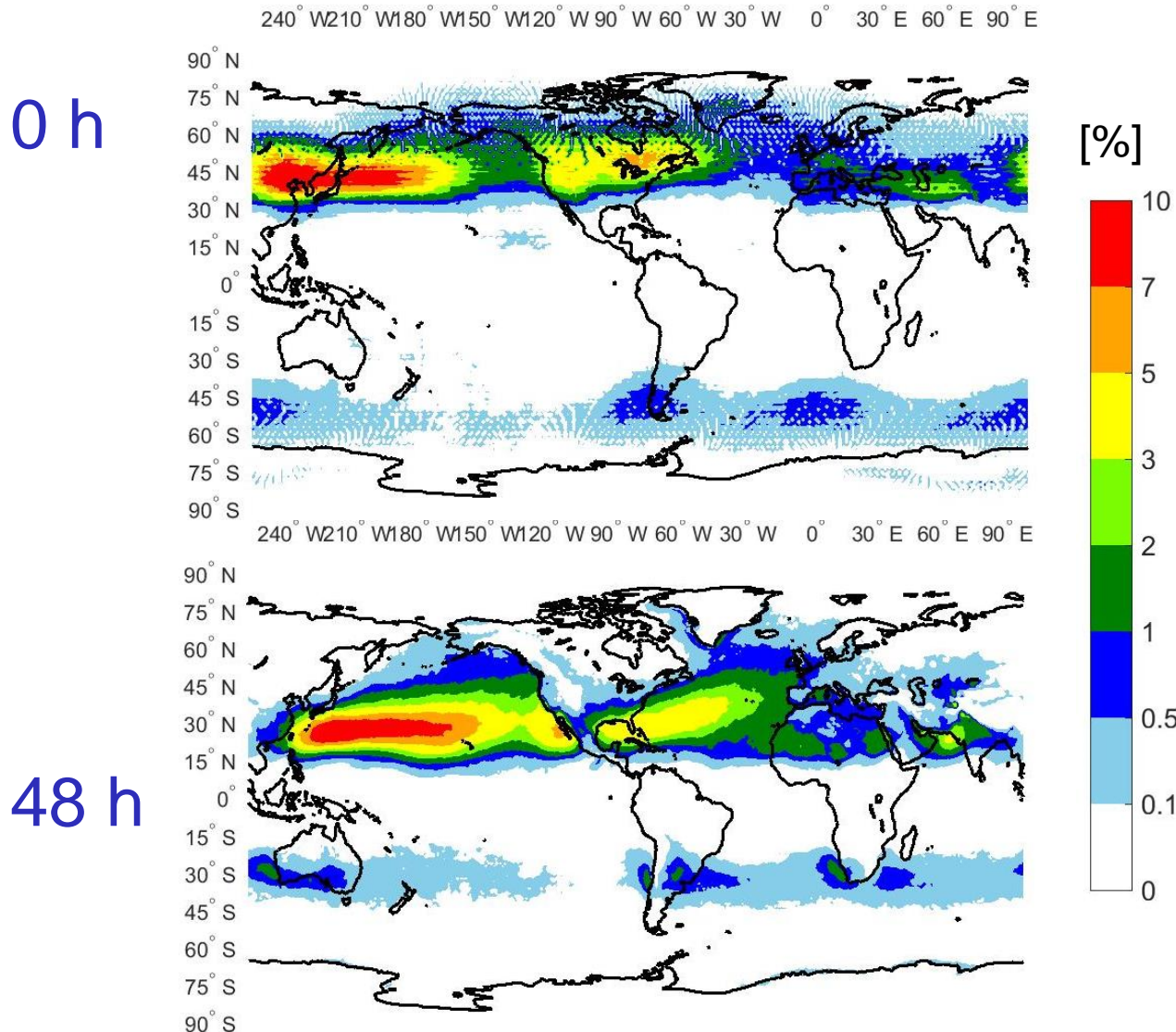
400-hPa descent in 48 h



- Forward trajectories start from a 3-D global grid every 6 h

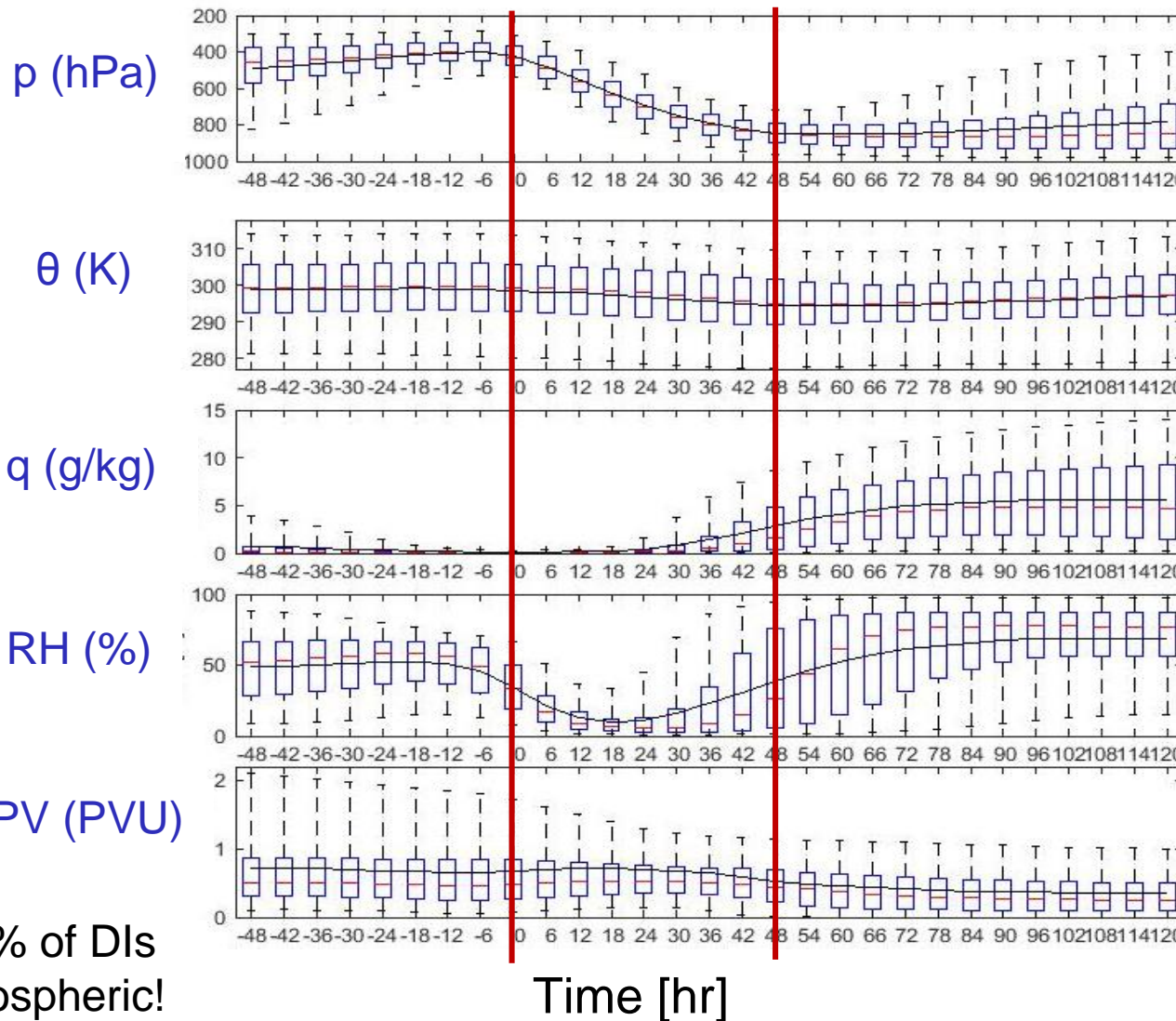
Raveh-Rubin, S., 2017: Dry intrusions: Lagrangian climatology and dynamical impact on the planetary boundary layer. *J. Climate*, doi: 10.1175/JCLI-D-16-0782.1

Dry intrusions: climatology DJF

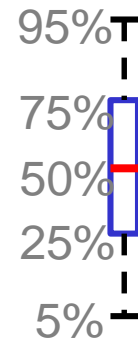


Raveh-Rubin, S., 2017: Dry intrusions: Lagrangian climatology and dynamical impact on the planetary boundary layer. *J. Climate*, doi: 10.1175/JCLI-D-16-0782.1

Dry intrusions: evolution



$26.6 \cdot 10^6$
trajectories



Raveh-Rubin, S., 2017: Dry intrusions: Lagrangian climatology and dynamical impact on the planetary boundary layer. *J. Climate*, doi: 10.1175/JCLI-D-16-0782.1

1. Feature-based diagnostics: website

<http://eraiclim.ethz.ch/>

Sprenger, M., G. Fragkoulidis, et al.: Global climatologies of Eulerian and Lagrangian flow features based on ERA-Interim reanalyses. *Bull. Amer. Meteor. Soc.* [doi:10.1175/BAMS-D-15-00299.1](https://doi.org/10.1175/BAMS-D-15-00299.1), in press.

Feature-based ERA-Interim Climatologies

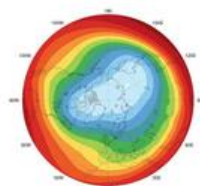
This collection of ERA-Interim based global climatologies of Eulerian and Lagrangian flow features is based on past and ongoing research of the Atmospheric Dynamics group at ETH Zürich. This webpage offers you access to monthly or longer-term averaged global fields from these climatologies. You can download netCDF, png or pdf files for the desired time period. The available fields span the period from January 1979 until (currently) February 2014.

Reference for the ERA-Interim dataset:

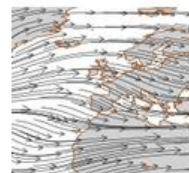
Dee, D. P. and coauthors, 2011: The ERA-Interim reanalysis: Configuration and performance of the data assimilation system, Quarterly Journal of Royal Meteorological Society, 137, 553–597, DOI:10.1002/qj.828.

Reference for the feature climatologies:

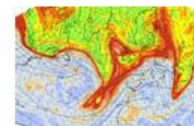
Sprenger, M., G. Fragkoulidis, H. Binder, M. Croci-Maspoli, P. Graf, C. M. Grams, P. Knippertz, E. Madonna, S. Schemm, B. Škerlak, and H. Wernli: Global climatologies of Eulerian and Lagrangian flow features based on ERA-Interim reanalyses. Bull. Amer. Meteor. Soc. doi:10.1175/BAMS-D-15-00299.1, in press.



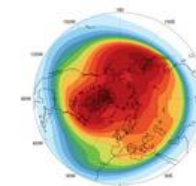
Pot. Temperature (TH)



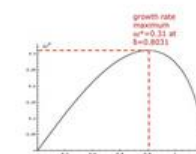
Wind Velocity



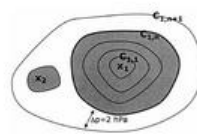
Pot. Vorticity (PV)



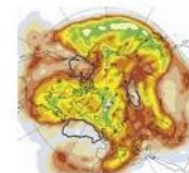
Tropopause Pressure



Eady Growth Rate



Cyclones / Anticyclones



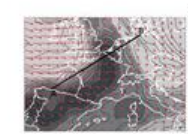
Atmospheric Blocks



PV Streamers



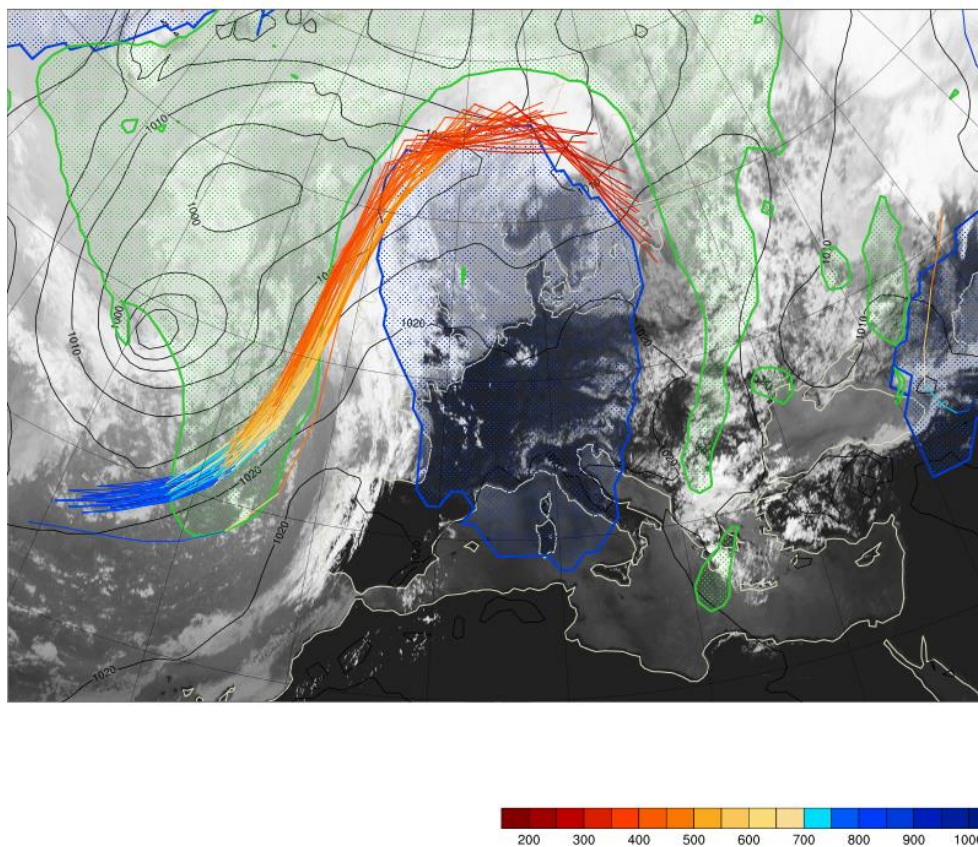
PV Cutoffs



Fronts

<http://eraiclim.ethz.ch/>

2. Diabatic influences on blocking

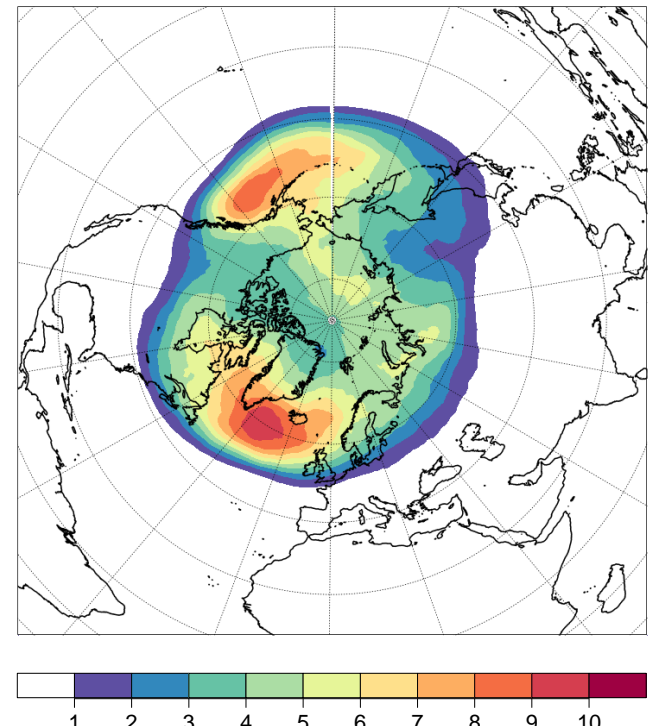


Pfahl, S., C. Schwierz, M. Croci-Maspoli, C. M. Grams, and H. Wernli, 2015: Importance of latent heat release in ascending air streams for atmospheric blocking. *Nature Geosci*, **8**, 610–614, [doi:10.1038/ngeo2487](https://doi.org/10.1038/ngeo2487).

Diabatic influence on blocking

Pfahl, S., et al. (2015), *NatGeo*, doi:10.1038/ngeo2487.

- Analyze ERA-Interim reanalysis data for the period 1989-2009.
- Identify **atmospheric blocking** as temporally persistent negative potential vorticity anomalies in the middle/upper troposphere (Schwierz et al., 2004).
- Calculate 7-day **backward trajectories** from grid points within blocking anticyclones.



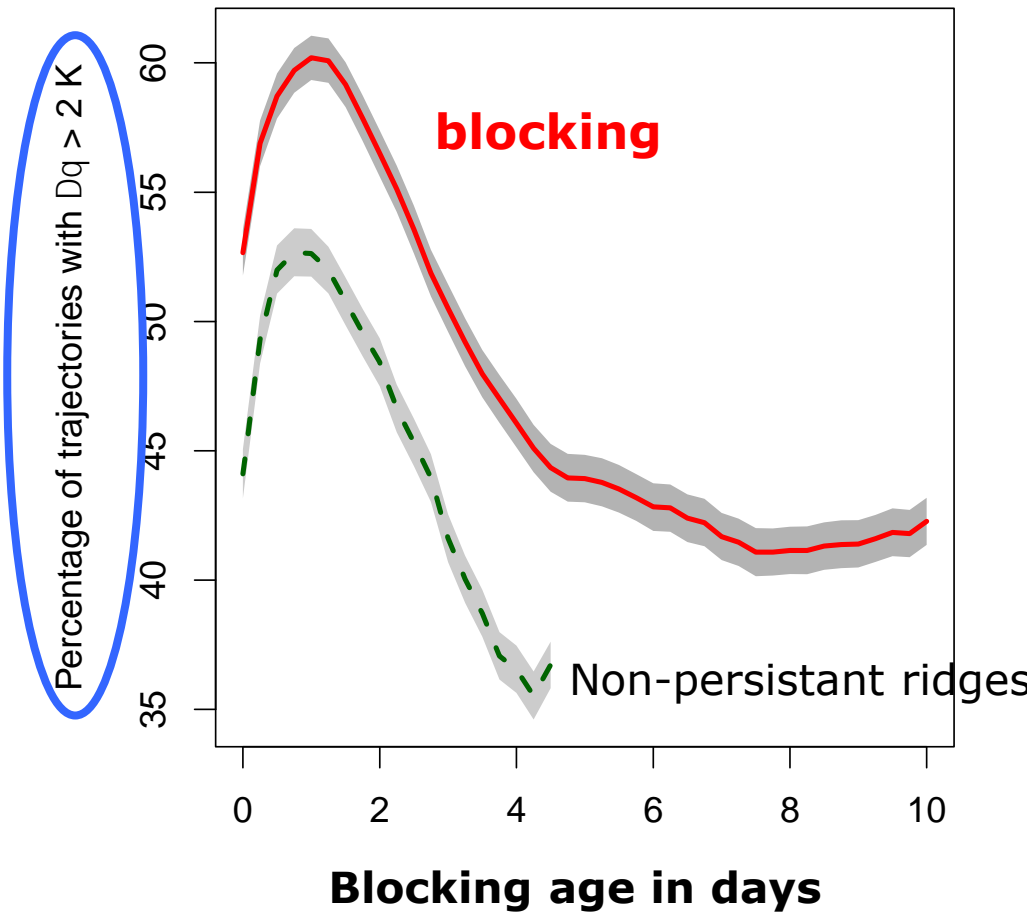
Annual mean blocking frequency (%).

slides by Stephan Pfahl

Diabatic heating and PV anomalies

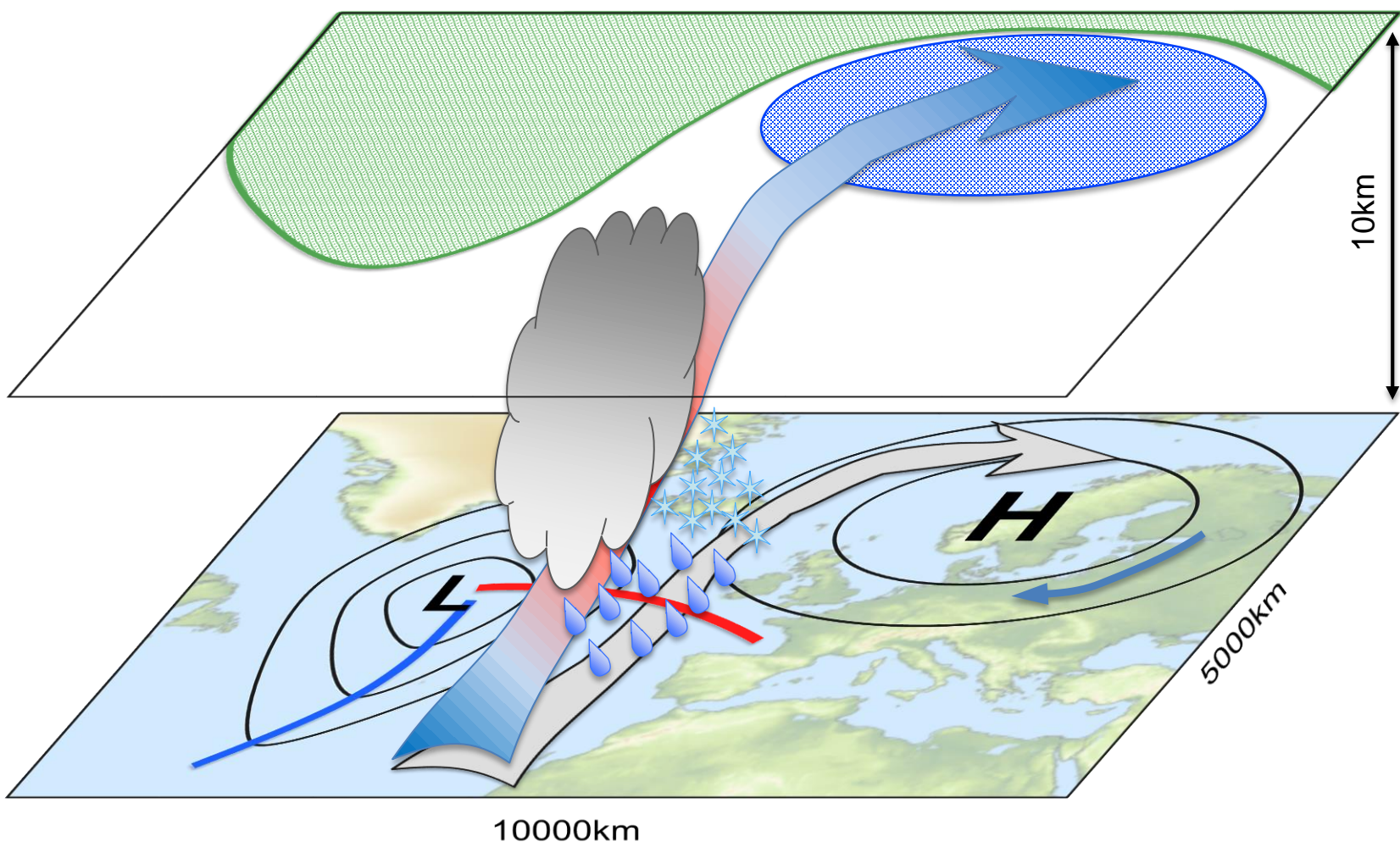
Pfahl, S., et al. (2015), *NatGeo*, doi:10.1038/ngeo2487.

**Diabatic heating
during 3 days
before arriving
in the blocking
region**



slides by Stephan Pfahl

Summary diabatic outflow and blocking



3. Operational forecast products

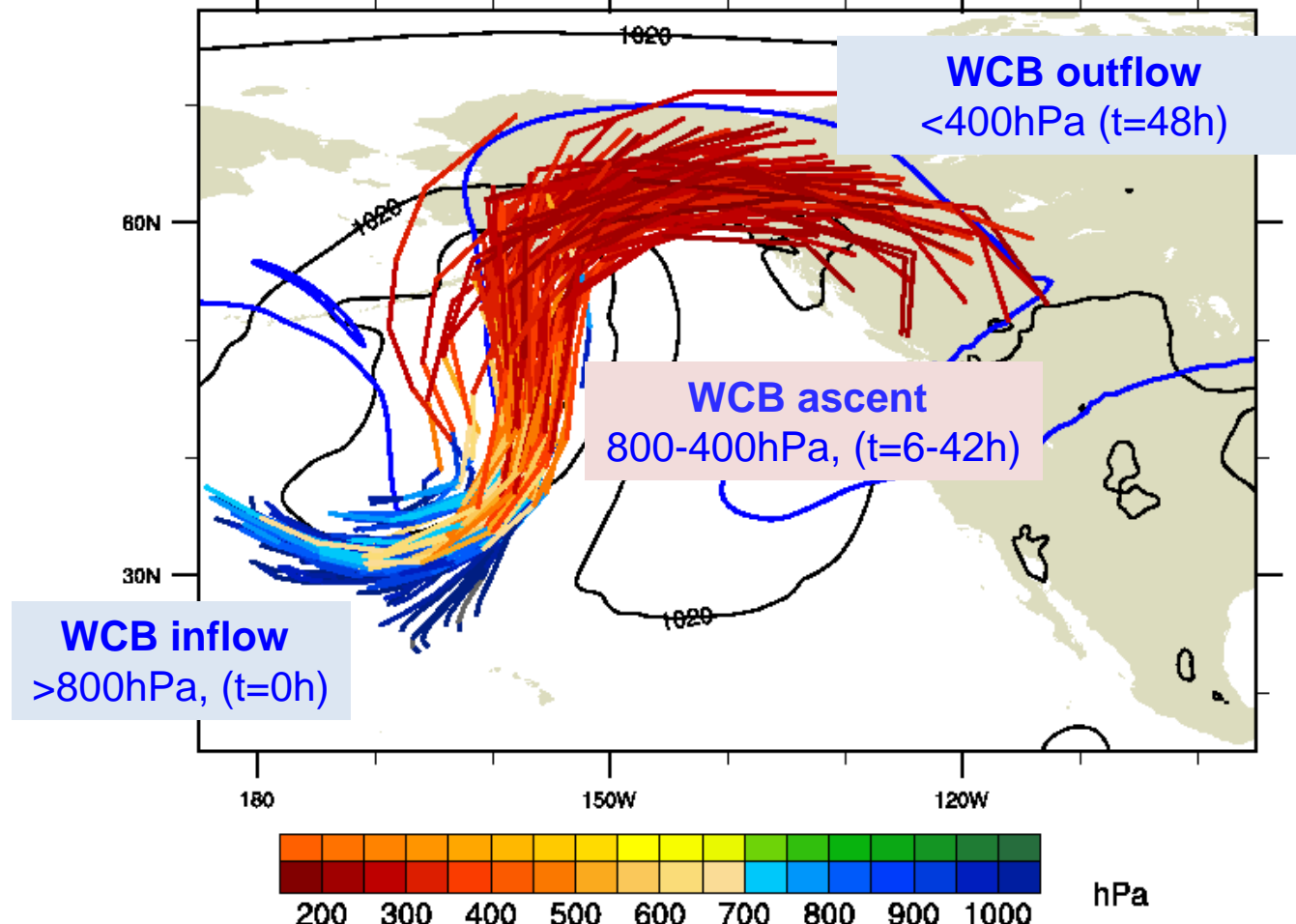
https://data.iac.ethz.ch/ml_cirrus/ec.ensemble/
(restricted access)

Schäfler, A., M. Boettcher, C. M. Grams, M. Rautenhaus, H. Sodemann, and H. Wernli, 2014: Planning aircraft measurements within a warm conveyor belt. *Weather*, **69**, 161–166, [doi:10.1002/wea.2245](https://doi.org/10.1002/wea.2245).

Rautenhaus, M., C. M. Grams, A. Schäfler, and R. Westermann, 2015: Three-dimensional visualization of ensemble weather forecasts – Part 2: Forecasting warm conveyor belt situations for aircraft-based field campaigns. *Geosci. Model Dev.*, **8**, 2355–2377, [doi:10.5194/gmd-8-2355-2015](https://doi.org/10.5194/gmd-8-2355-2015).

Warm conveyor belts

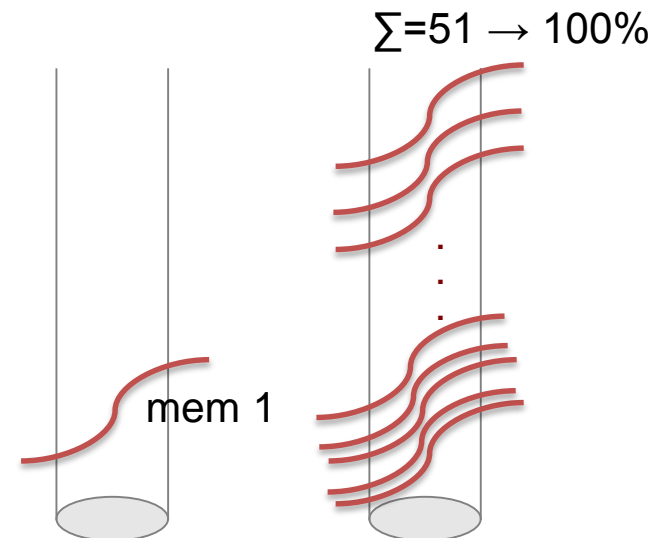
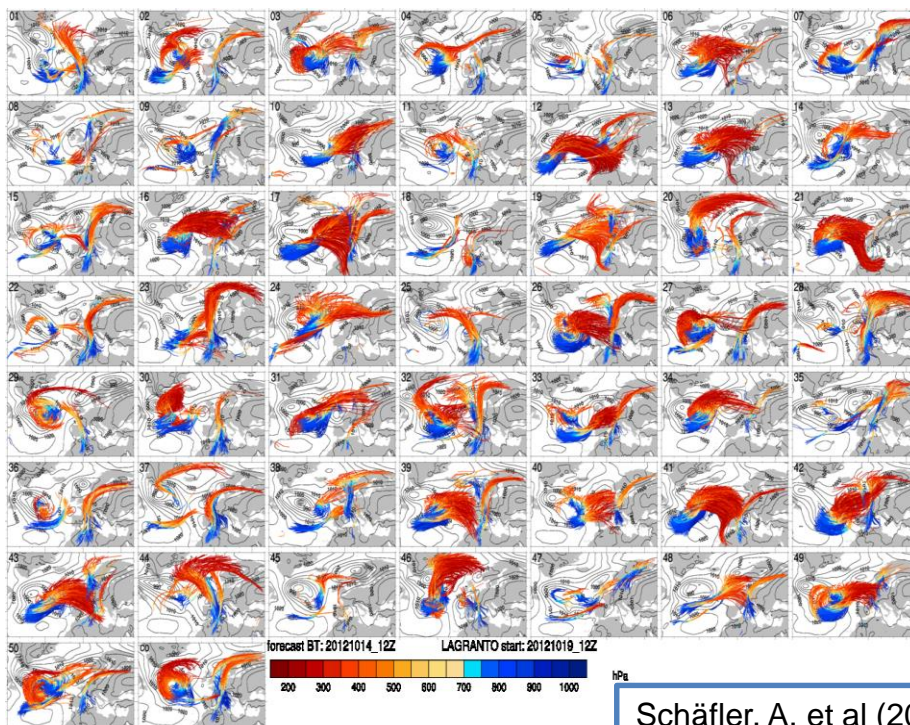
- operational ECMWF **high resolution** forecast
- **model level data** +0h to +96h every 3h; +96h to +192h every 6h
- 48h forward trajectories $\Delta p/\Delta t \geq 600\text{hPa}/48\text{h}$



WCB ensemble forecast

- operational ECMWF **ensemble** forecast
- **model level data +0h to +168h every 6h**
- 48h forward trajectories $\Delta p/\Delta t \geq 550\text{hPa}/48\text{h}$

WCB calculations for each ECMWF ensemble member on ecgate

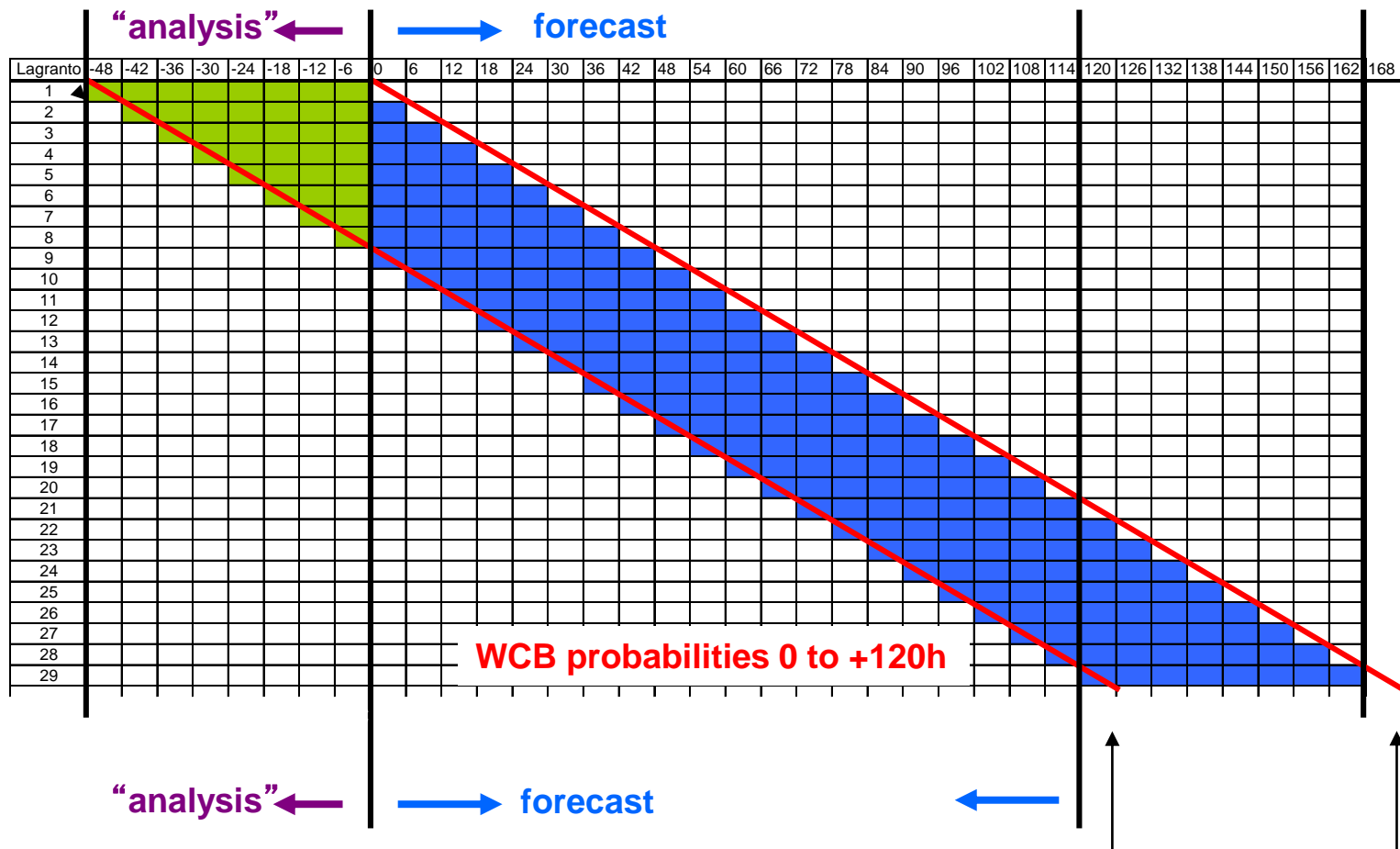


Schäfler, A. et al (2014), *Weather*, doi:10.1002/wea.2245.

Rautenhaus, M., C. Grams, et al. (2015), *GMD*, doi:10.5194/gmd-8-2355-2015.

WCB ensemble forecast

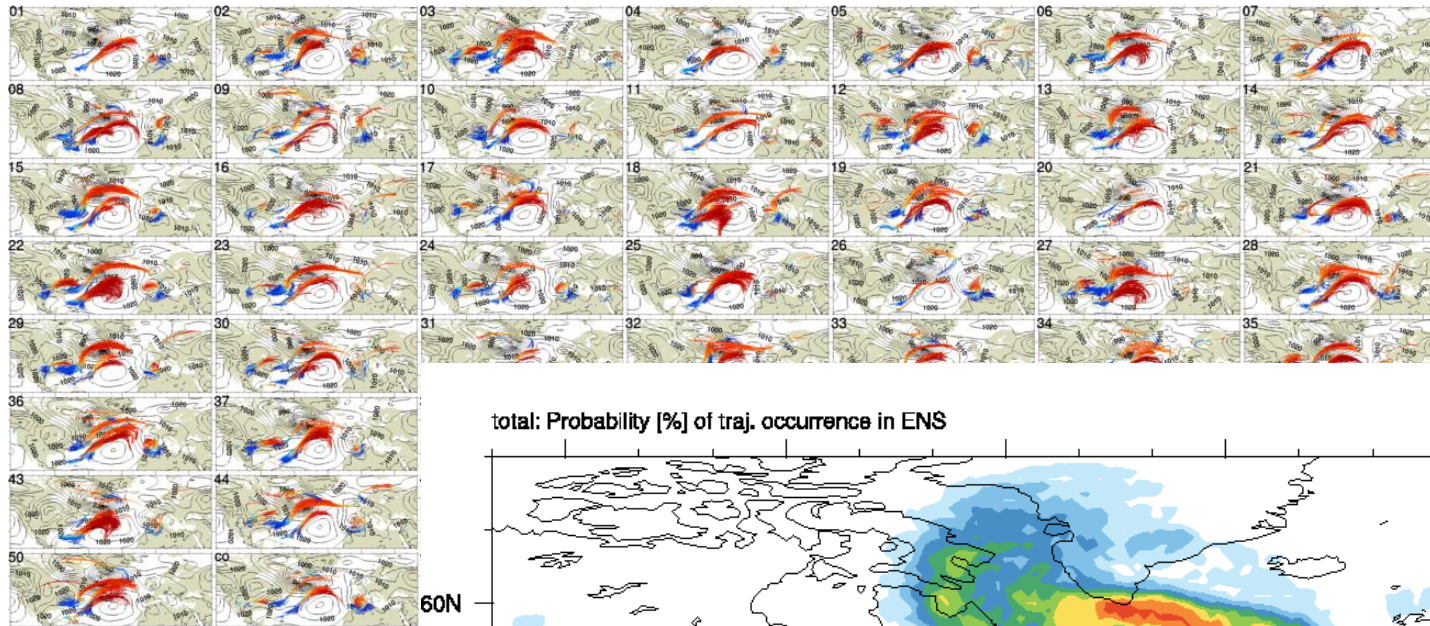
- Illustration of time-lagged Lagranto for **one** forecast



- at each fc time (0 to 120 hours) trajectories from 9 LAGRANTO calculations for one fc

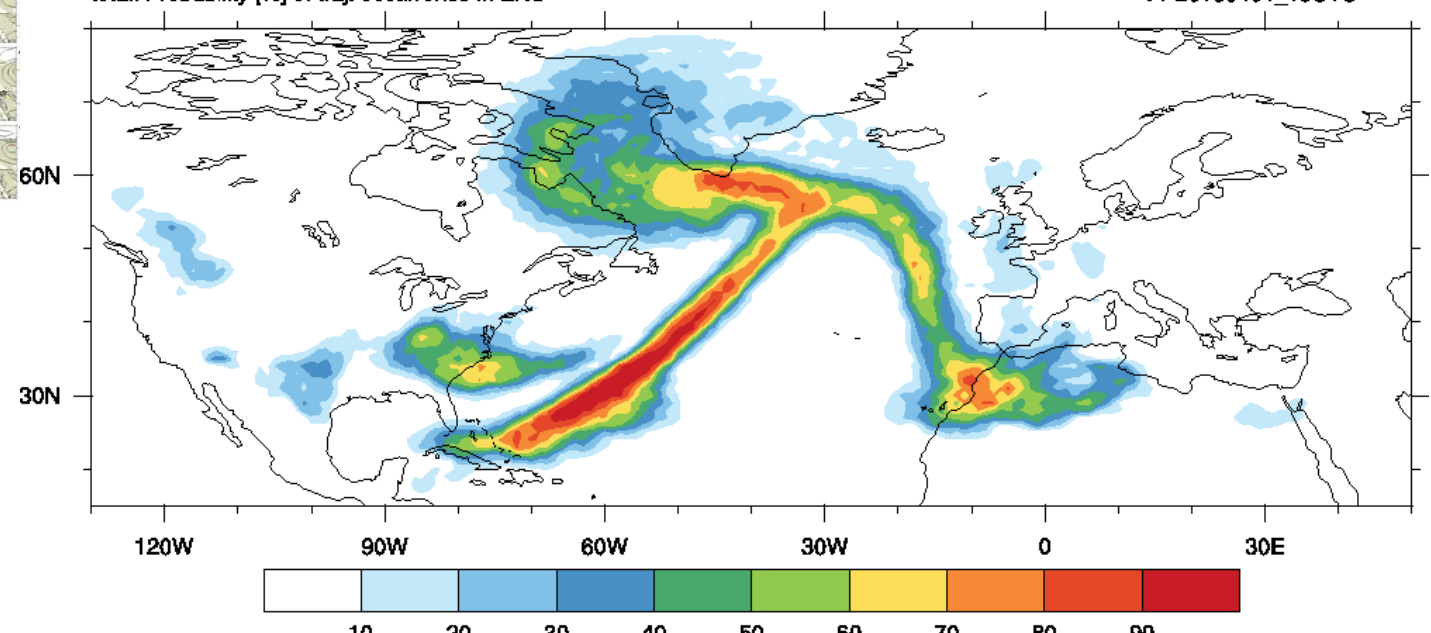
0h 48h
LAGRANTO time

WCB ensemble forecast



Probabilities for different layers:

- Total
- Outflow
- Ascent
- Inflow



Schäfler, A. et al (2014), *Weather*, doi:10.1002/wea.2245.

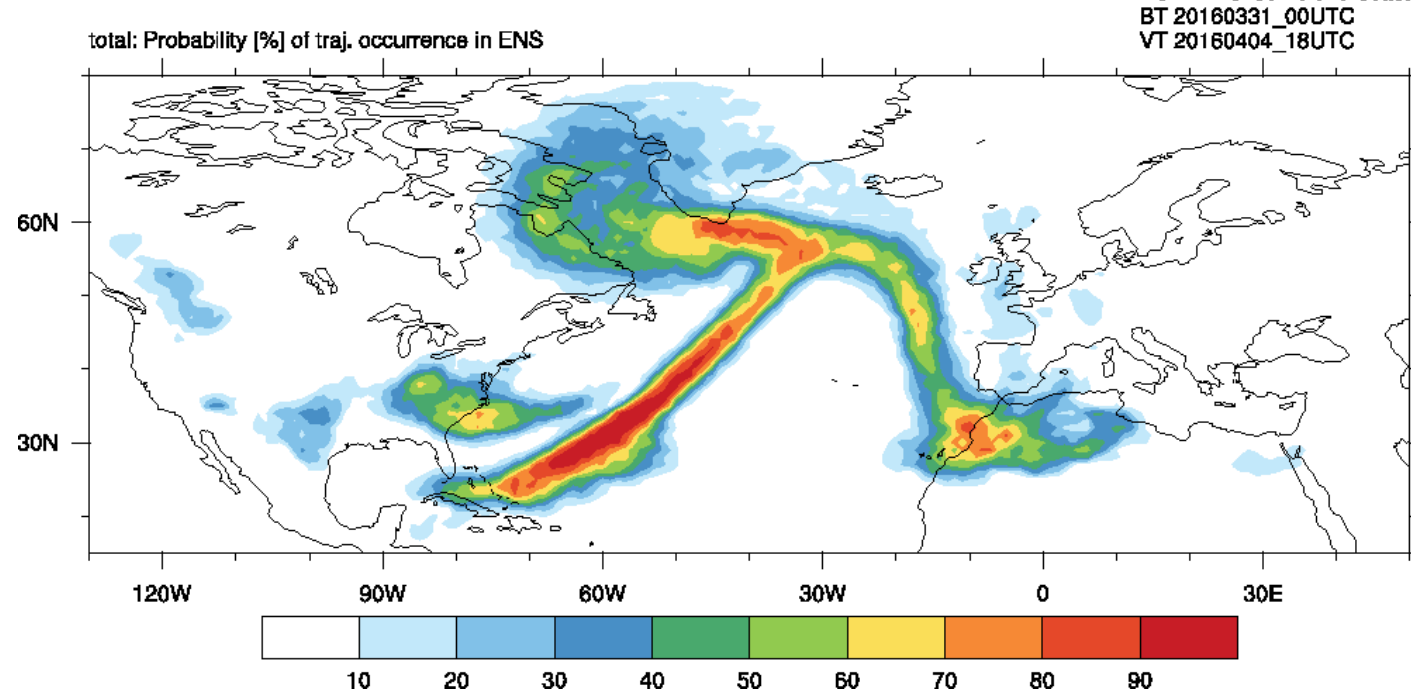
Rautenhaus, M., C. Grams, et al. (2015), *GMD*, doi:10.5194/gmd-8-2355-2015.

WCB ensemble forecast

WCB probability BT 20160331_00 VT +114h 20160404_18

Total column

- Forecast product: **probability of WCB occurrence**



M: mask indicating if ($M=1$) or if not ($M=0$) ens mem. e has a traj at (i,j)
E: number of ens. members (=51)
 i,j : index of gridpoint (i,j)
 e : index of ensemble member e

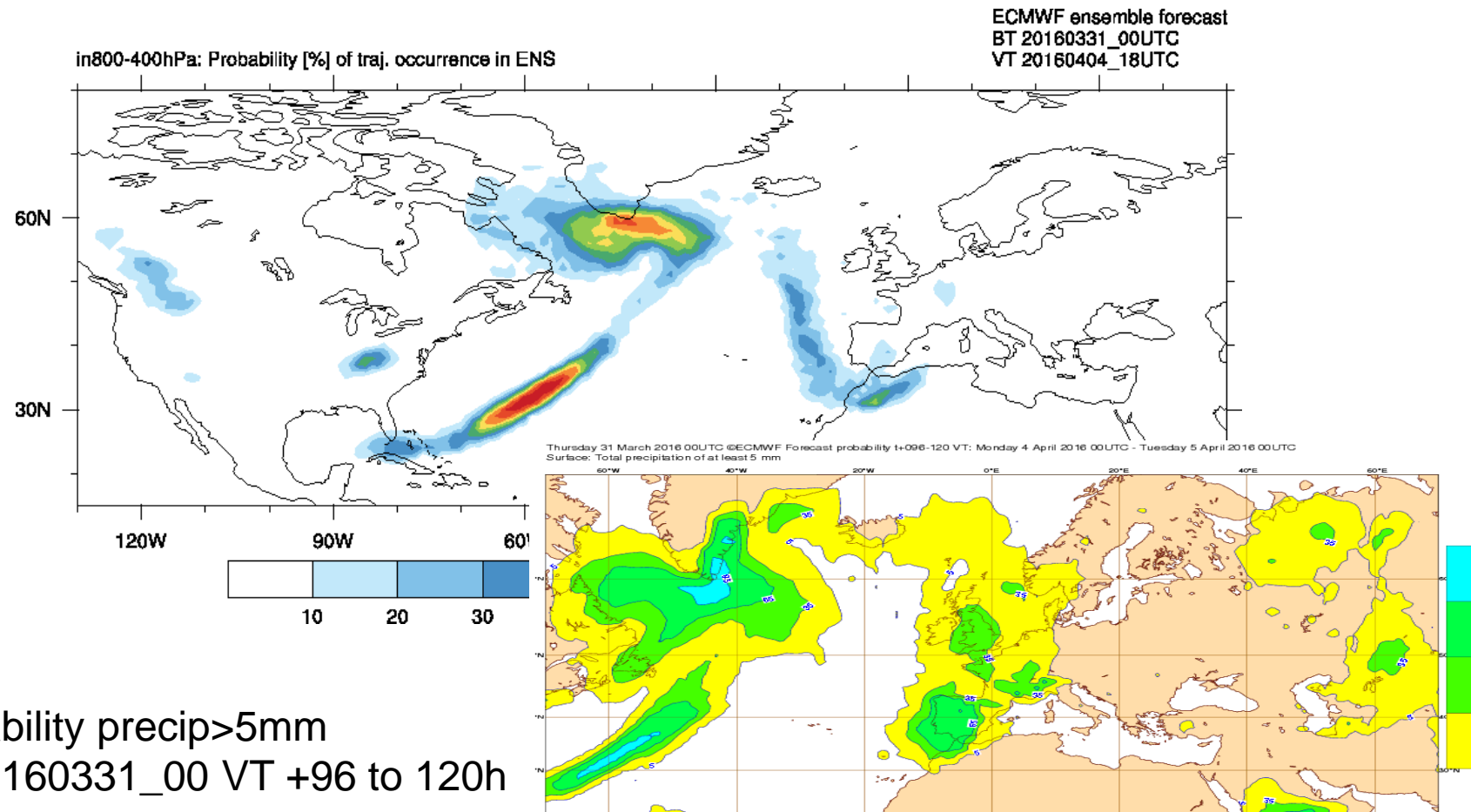
$$\frac{1}{E} \sum_e M_{i,j}^e$$

Schäfler, A. et al (2014), *Weather*, doi:10.1002/wea.2245.

Rautenhaus, M., C. Grams, et al. (2015), *GMD*, doi:10.5194/gmd-8-2355-2015.

WCB ensemble forecast

WCB probability BT 20160331_00 VT +114h 20160404_18
Ascent (800-400hPa)

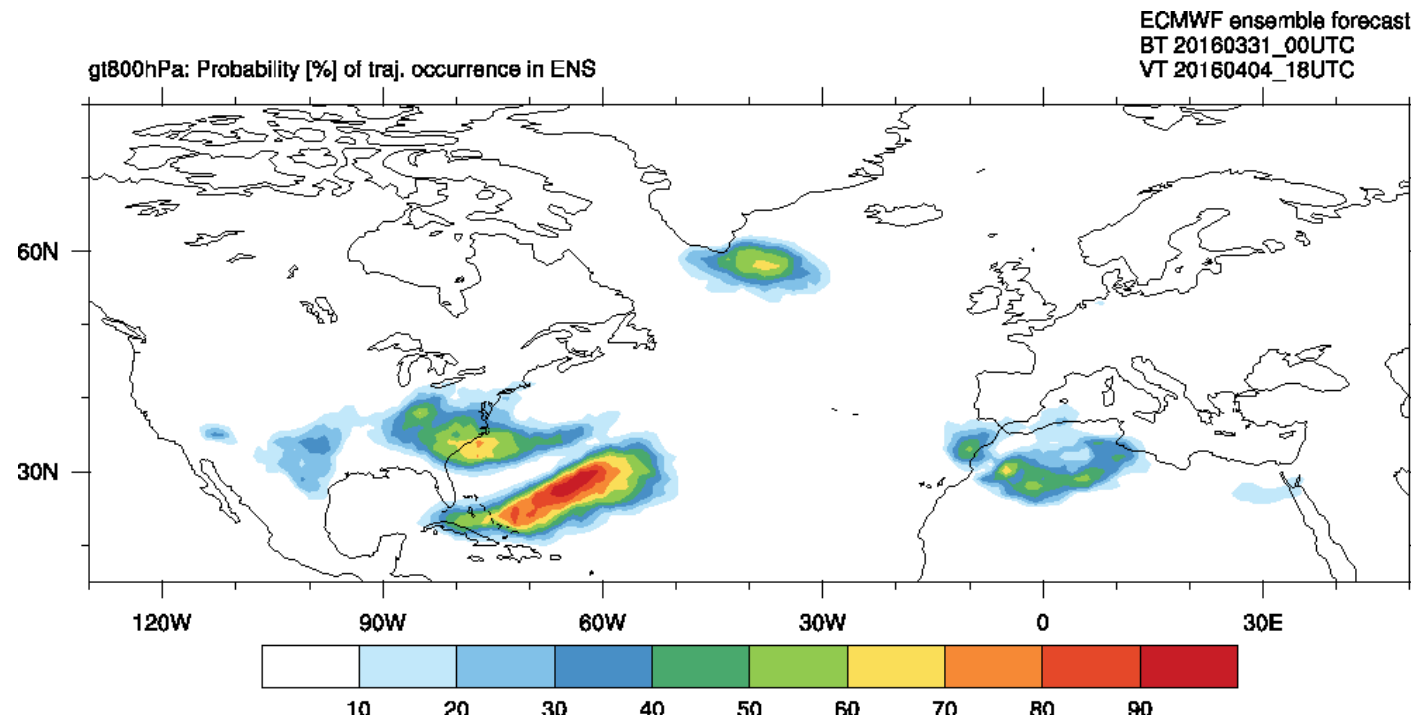


Schäfler, A. et al (2014), *Weather*, doi:10.1002/wea.2245.

Rautenhaus, M., C. Grams, et al. (2015), *GMD*, doi:10.5194/gmd-8-2355-2015.

WCB ensemble forecast

WCB probability BT 20160331_00 VT +114h 20160404_18
Inflow (>800hPa)



Schäfler, A. et al (2014), *Weather*, doi:10.1002/wea.2245.

Rautenhaus, M., C. Grams, et al. (2015), *GMD*, doi:10.5194/gmd-8-2355-2015.

WCB ensemble forecast

Demonstration of current forecast products:

- High resolution forecast
- Ensemble forecast
- (crosstool)

https://data.iac.ethz.ch/ml_cirrus/ec.ensemble/

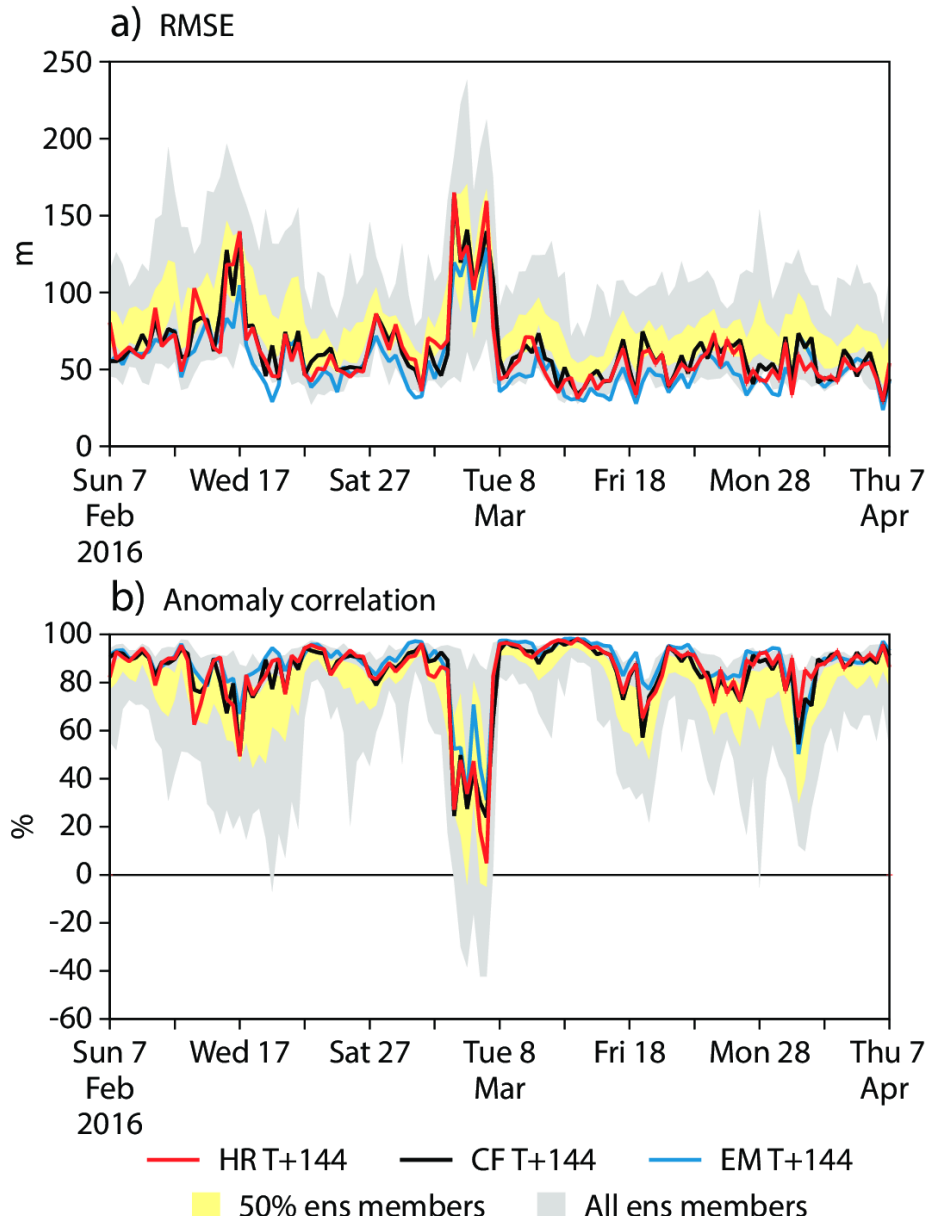
(restricted access)

4. A recent forecast bust

Madonna, E., M. Boettcher, C. M. Grams, H. Joos, O. Martius, and H. Wernli, 2015: Verification of North Atlantic warm conveyor belt outflows in ECMWF forecasts. *Q.J.R. Meteorol. Soc.*, **141**, 1333–1344, [doi:10.1002/qj.2442](https://doi.org/10.1002/qj.2442).

Grams, C.M., L. Magnusson, and E. Madonna, 2017: An atmospheric dynamics' perspective on the amplification and propagation of forecast error in numerical weather prediction models: a case study. *In preparation for QJRMS*

00UTC 7 March 2016 forecast bust



Z500 RMSE and
ACC for HRES and
ENS - Europe

Plots by Linus
Magnusson (ECMWF)

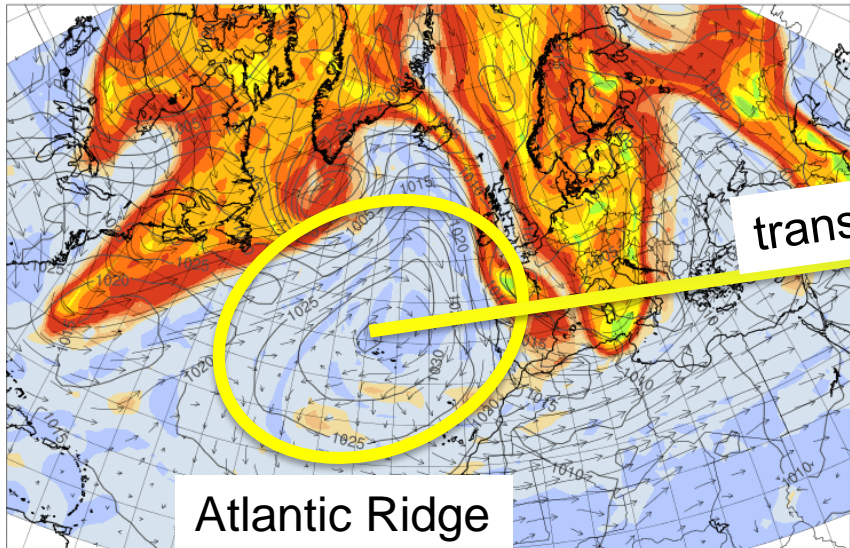
Synoptic evolution

AR to **BL** transition from **20160307_00** to **20160308_18**

ECMWF analysis

PV@315K, 00 UTC 7 March

PV@315K at 20160307_00

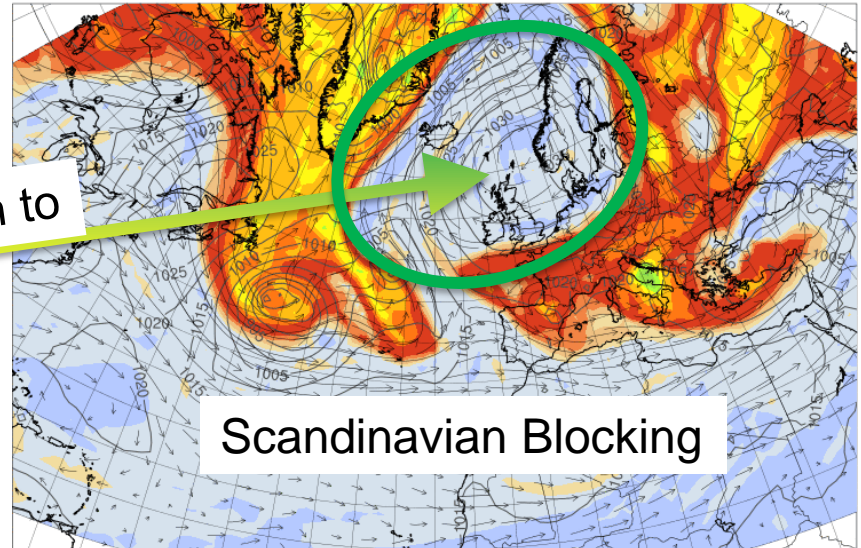


Atlantic Ridge



PV@315K, 12UTC 14 March

PV@315K at 20160314_12



Scandinavian Blocking

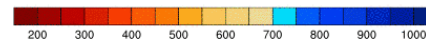
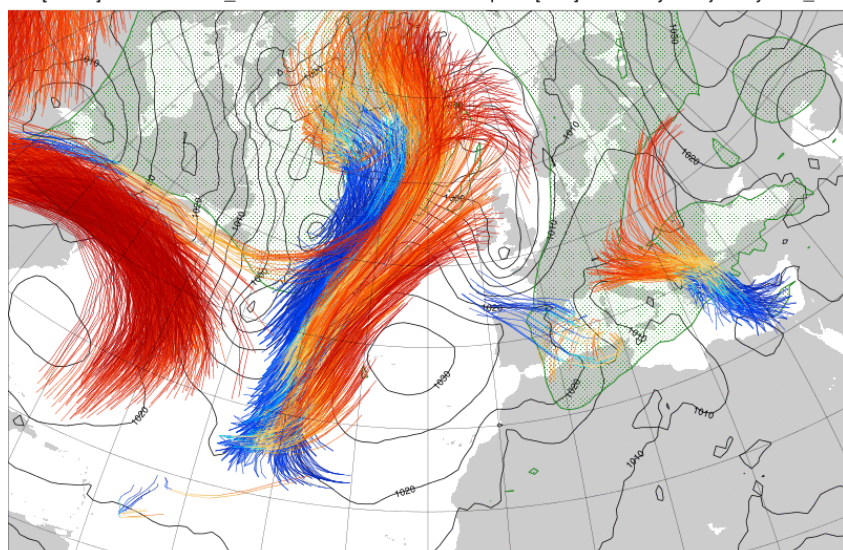


Synoptic evolution

AR to **BL** transition from **20160307_00** to **20160308_18**

ECMWF analysis

ECMWF analysis BT: 20160309_00Z
LAGRANTO start and PMSL VT: 20160309_00Z
IPV [2PVU] VT: 20160311_00Z

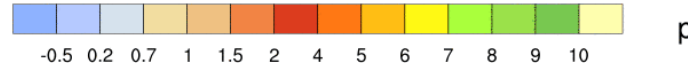
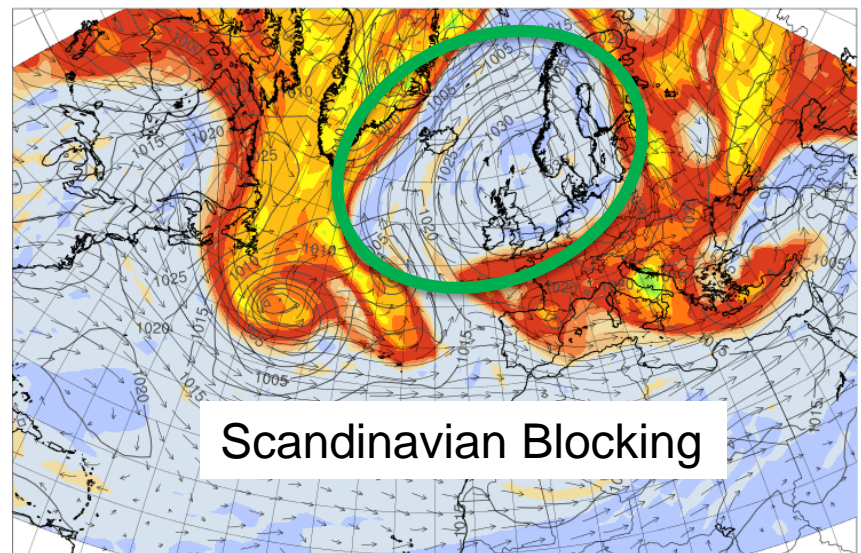


WCB

start 00 UTC 9 March → end 00 UTC 11 March
& PMSL
& PV@315K

PV@315K, 12UTC 14 March

PV@315K at 20160314_12

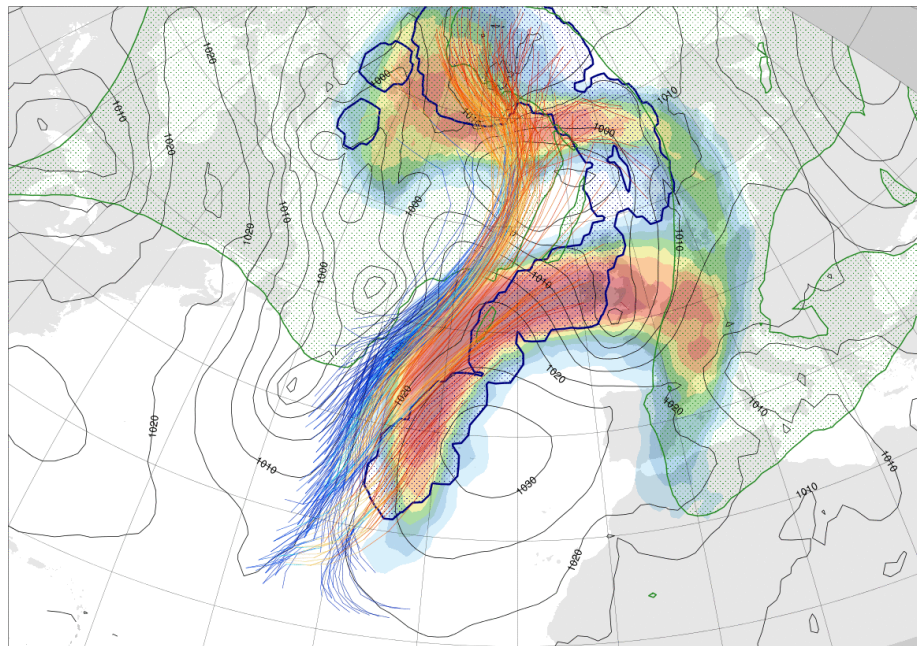


The PAL forecast metric

- Metric for quantifying the **PV**, **Amplitude**, and **Location** error of WCB outflow objects
- **P term:** <0, too weak / >0, too strong negative PV anomaly in outflow
- **A term:** <0, too few / >0 too many trajectories
- **L term:** 0 good; close to 2 → objects in opposite corners

ECMWF analysis BT: 20160309_00Z
LAGRANTO start and PMSL VT: 20160309_00Z
IPV[2PVU] VT: 20160311_00Z

pmsl [hPa] and every 1 trajectory
WCB region: 70W30W20N50N_t0

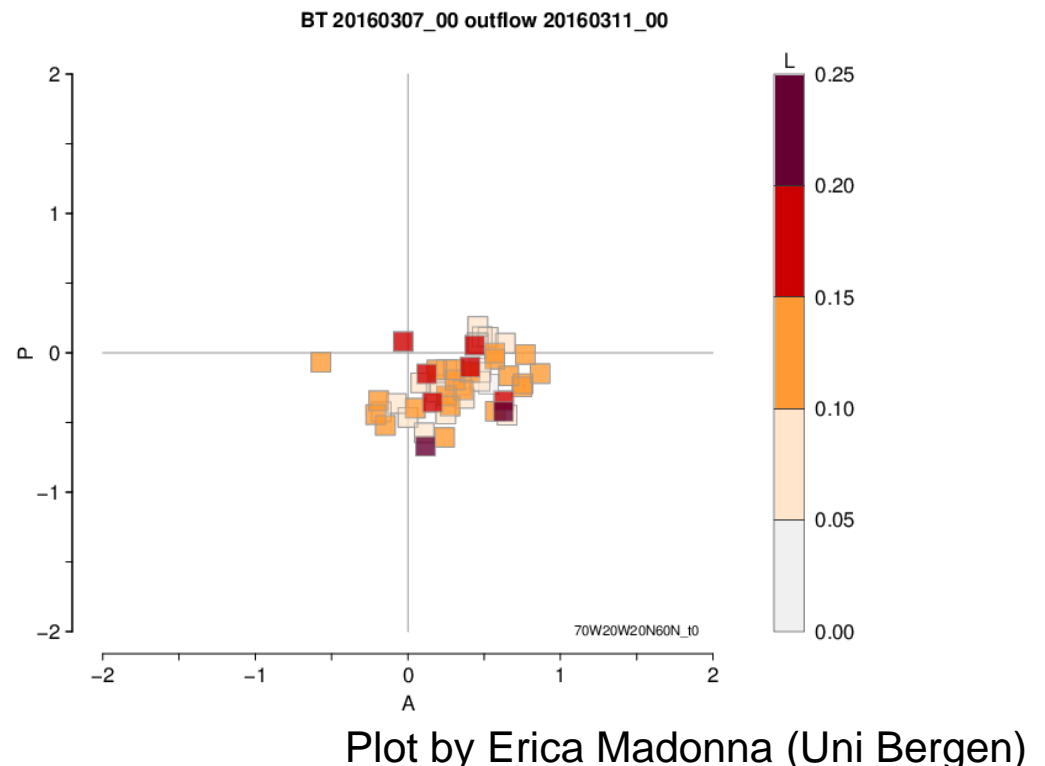


Madonna et al. (2014), QJRMS,
[doi:10.1002/qj.2442](https://doi.org/10.1002/qj.2442)

The PAL forecast metric

- Metric for quantifying the **PV**, **Amplitude**, and **Location** error of WCB outflow objects
- **P** term: <0, too weak / >0, too strong negative PV anomaly in outflow
- **A** term: <0, too few / >0 too many trajectories
- **L** term: 0 good; close to 2 → objects in opposite corners

PAL diagram illustrates the three components, for different forecast members



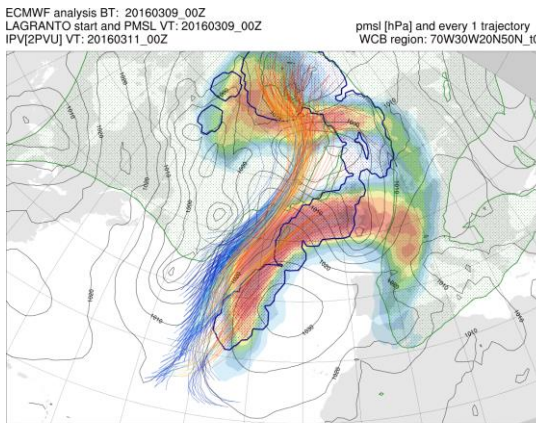
Madonna et al. (2014), QJRMS,
[doi:10.1002/qj.2442](https://doi.org/10.1002/qj.2442)

Role of WCB in forecast bust

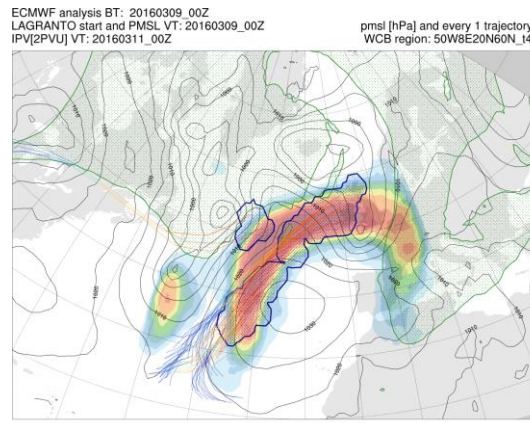
ECMWF ensemble initial time **20160307_00**

focus on WCB starting 00 UTC 9 March (+48h) → ending 00 UTC 11 March (+96h)

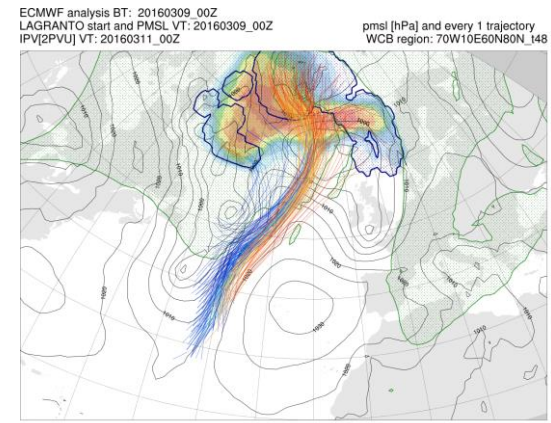
ALL



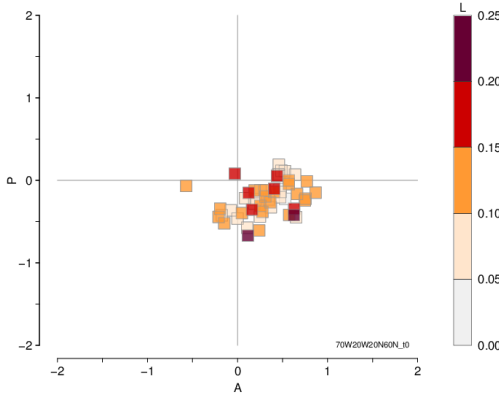
SOUTH



NORTH



BT 20160307_00 outflow 20160311_00

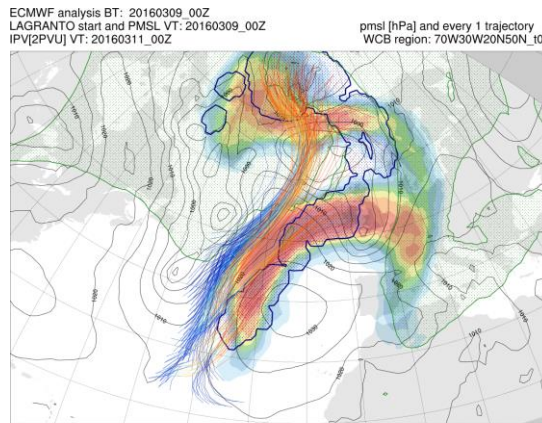


Role of WCB in forecast bust

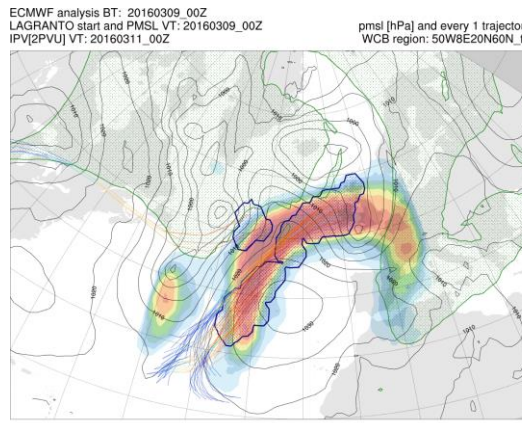
ECMWF ensemble initial time **20160307_00**

focus on WCB starting at **09_00Z (+48h)** → ending at **11_00Z (+96h)**

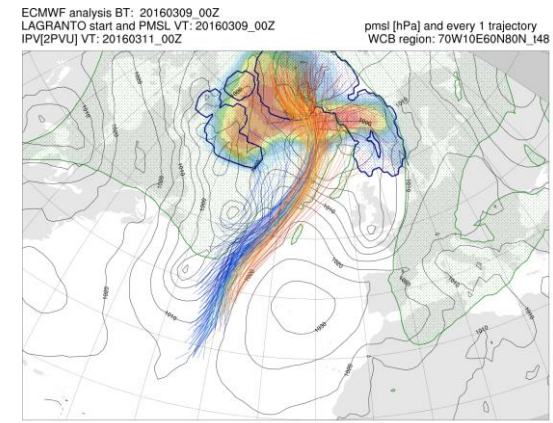
ALL



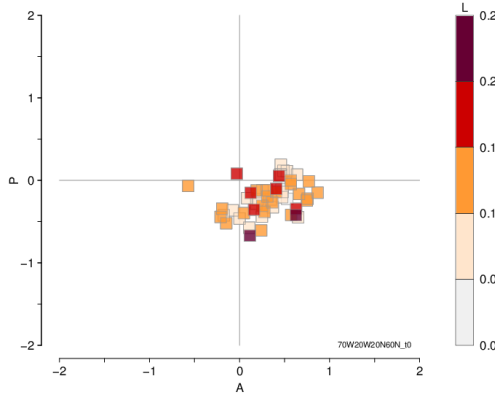
SOUTH



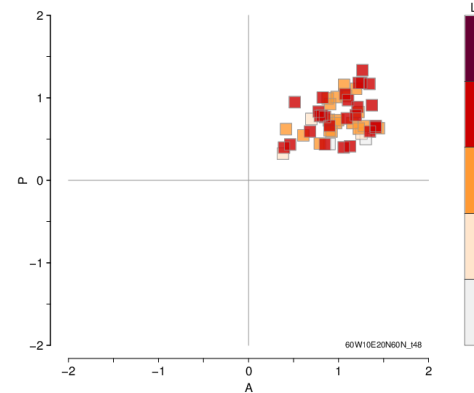
NORTH



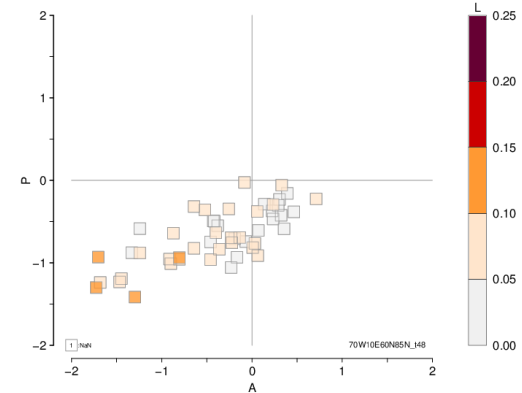
BT 20160307_00 outflow 20160311_00



BT 20160307_00 outflow 20160311_00

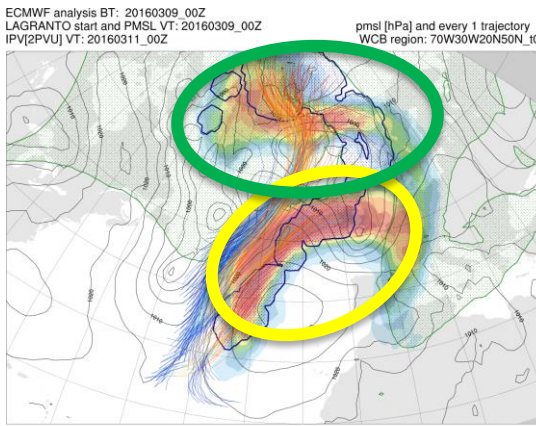


BT 20160307_00 outflow 20160311_00

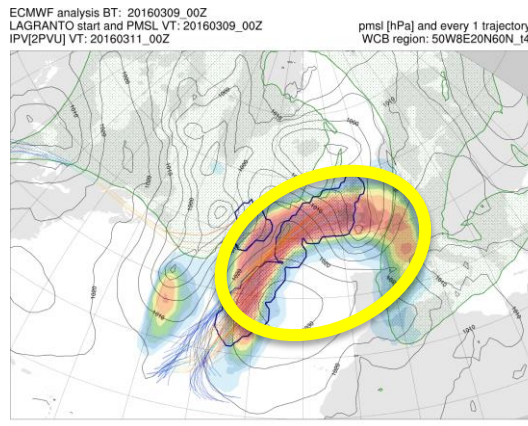


Role of WCB in forecast bust

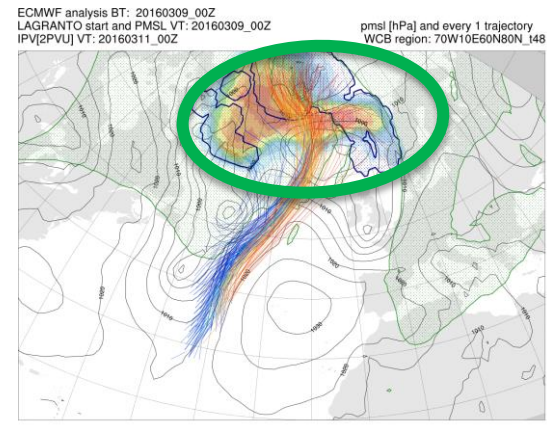
ALL



SOUTH

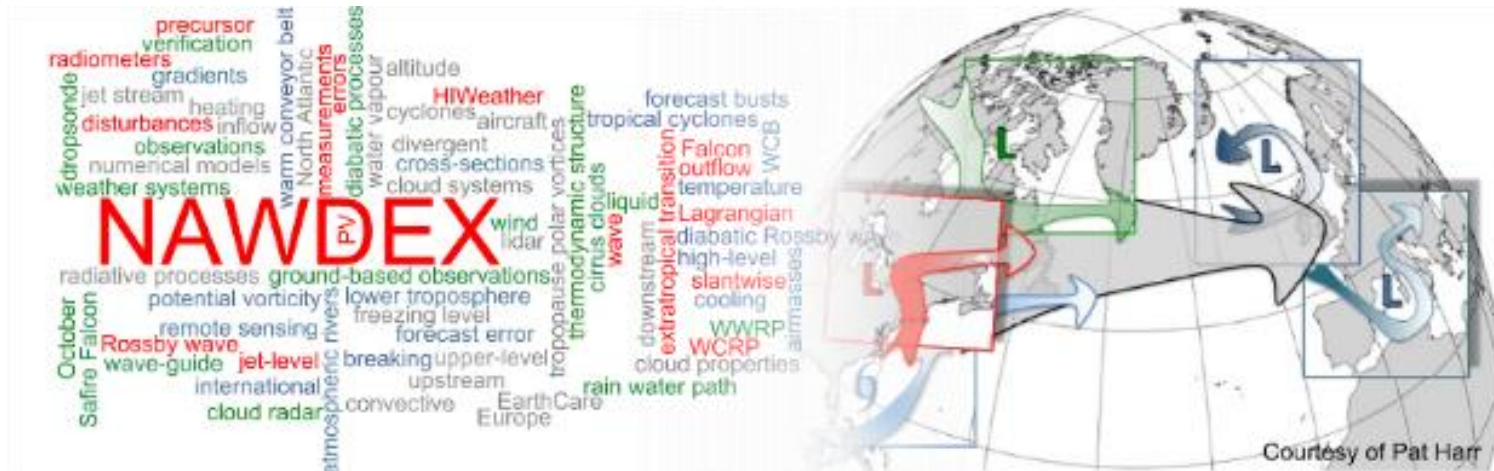


NORTH



- Southern WCB branch is too strong, rather maintains AR
- Northern branch is too weak, BL does not establish over Scandinavia

5. Demonstration NAWDEX



Demonstration of flight planning for IOP2 21 Sep 2016

<http://nawdex.ethz.ch/>

<https://data.iac.ethz.ch/nawdex/index.php>
(restricted access)

NAWDEX IOP2

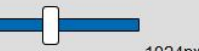
NAWDEX ETH Products

Select Date: 2016-09-22 0 Submit

Or select a specific case: IOP2: Ursula

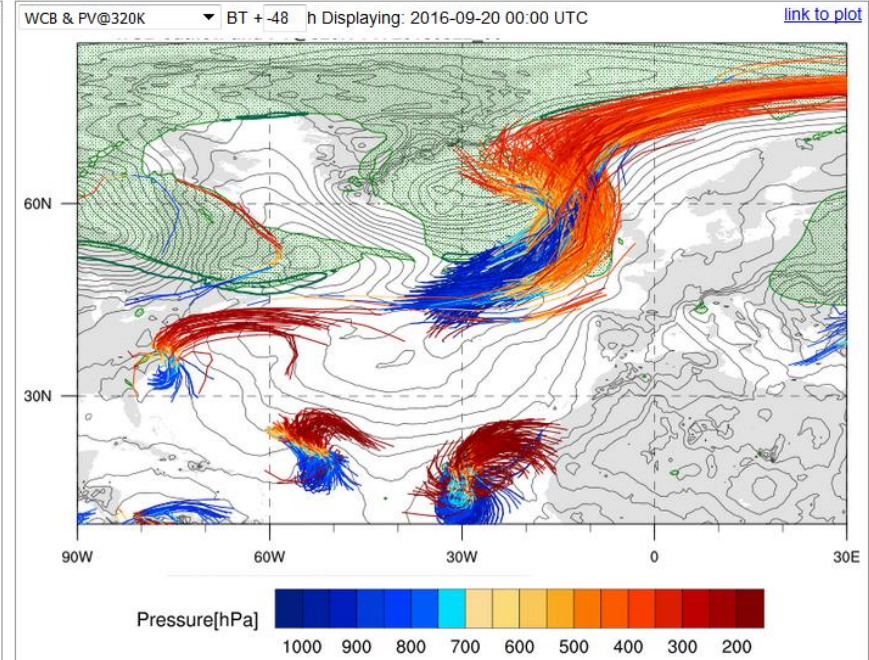
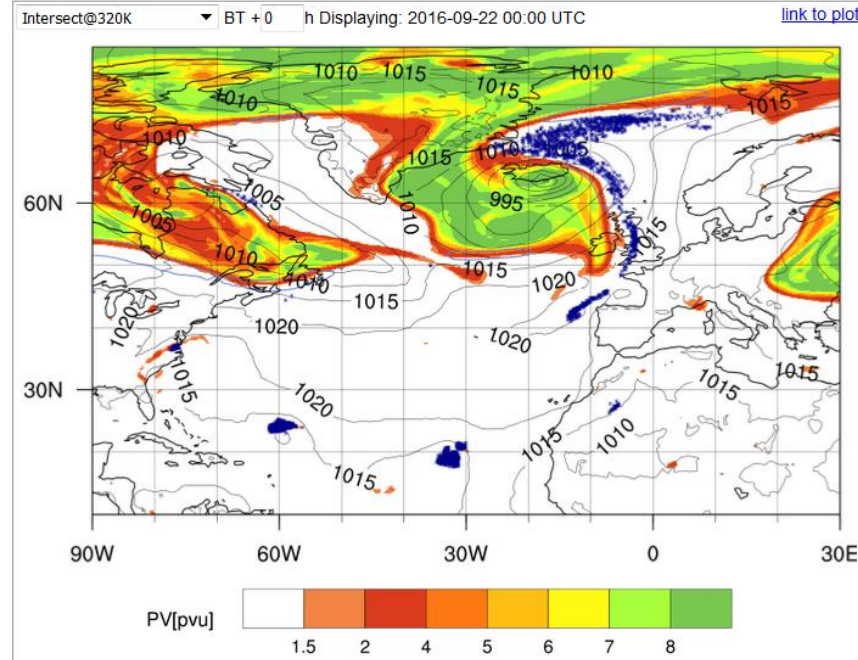
-12h -6h -1h +1h +6h +12h

Width: 400px



delete plot

add plot



Keyboard shortcuts:

- ↑ increase time by 1h
- ↓ decrease time by 1h
- ↗ increase time by 12h
- ↘ decrease time by 12h
- Num + increase plot size
- Num - decrease plot size
- a add plot
- d delete plot

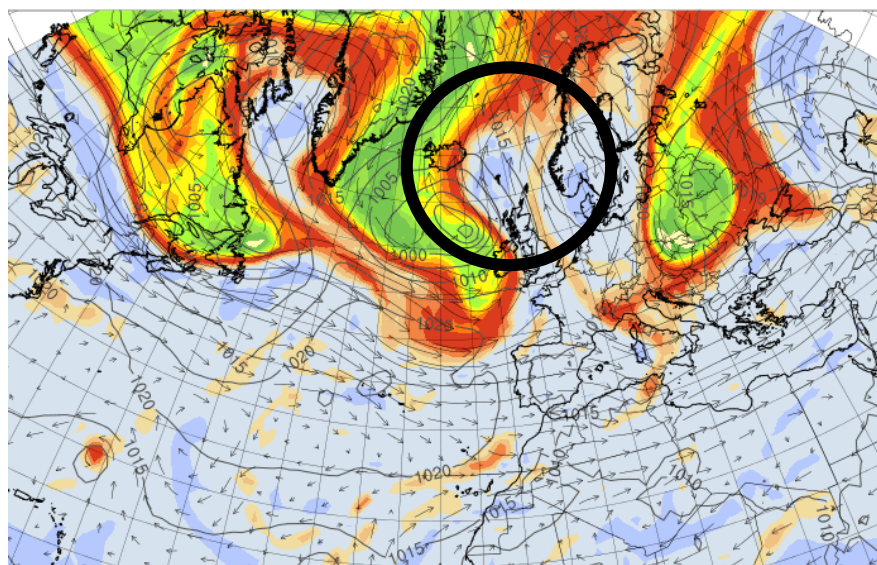
Report any bugs/feedback to: roman.attinger(at)env.ethz.ch

Last updated: 03.03.2017

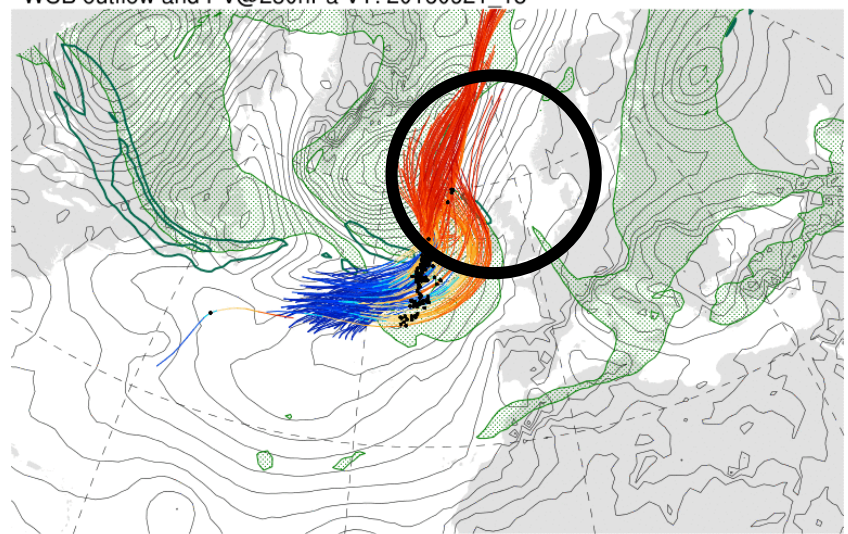
<https://data.iac.ethz.ch/nawdex/index.php>
(restricted access)

Roman Attinger, Maxi Böttcher, Julian Quinting

PV@325K at 20160921_18



Trajectory start and SLP VT: 20160919_18
WCB outflow and PV@250hPa VT: 20160921_18

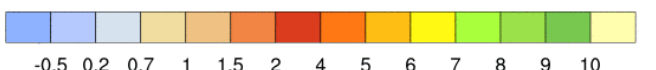
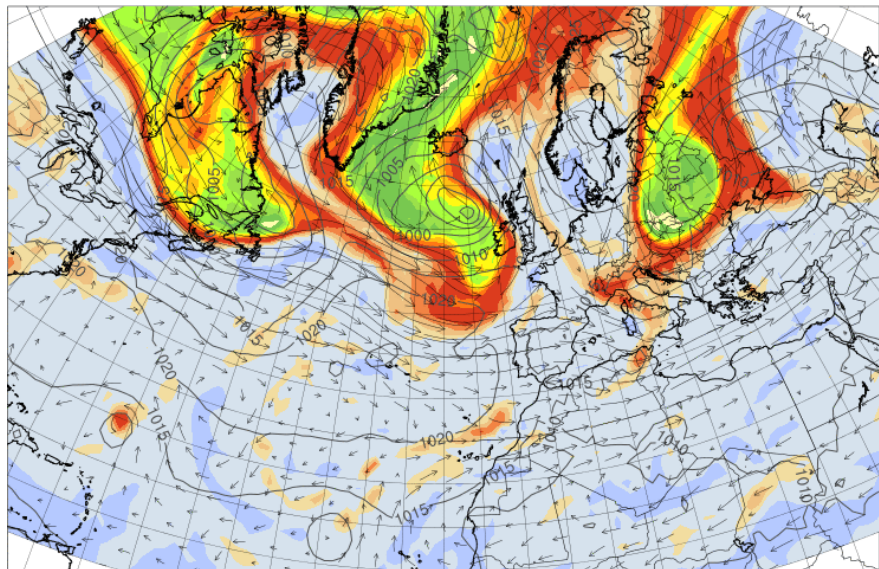


3 days before mission:

- Monitoring of evolution in **hres** and confirmation with **ensemble**

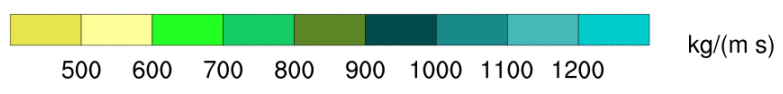
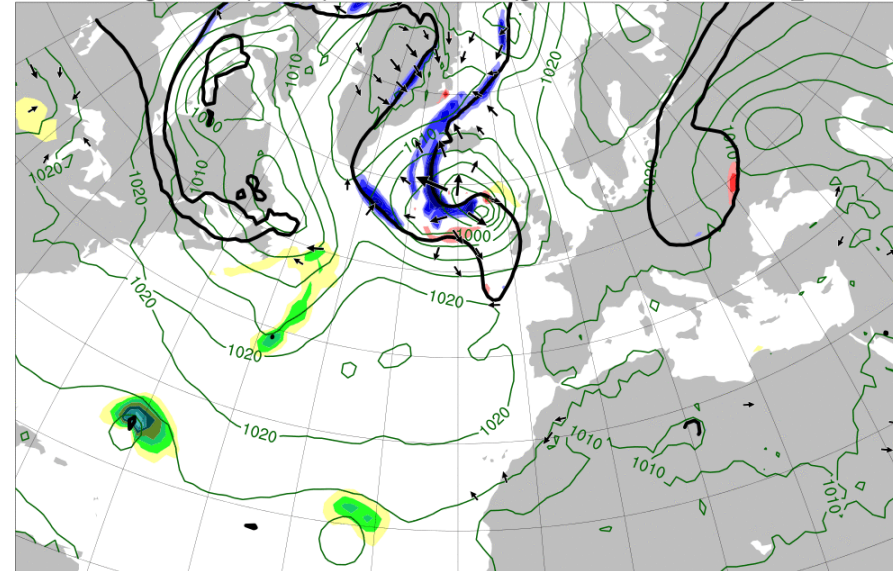
Maxi Böttcher and Julian Quinting

PV@325K at 20160921_18



pvu

2 PVU (black contour), PV advection through divergent wind (shading), divergent wind (vectors) @315K and MSLP (green contours) at 20160921_18



500 600 700 800 900 1000 1100 1200

kg/(m s)



-12 -10 -8 -6 -4 4 6 8 10 12

PVU/d

3 days before mission:

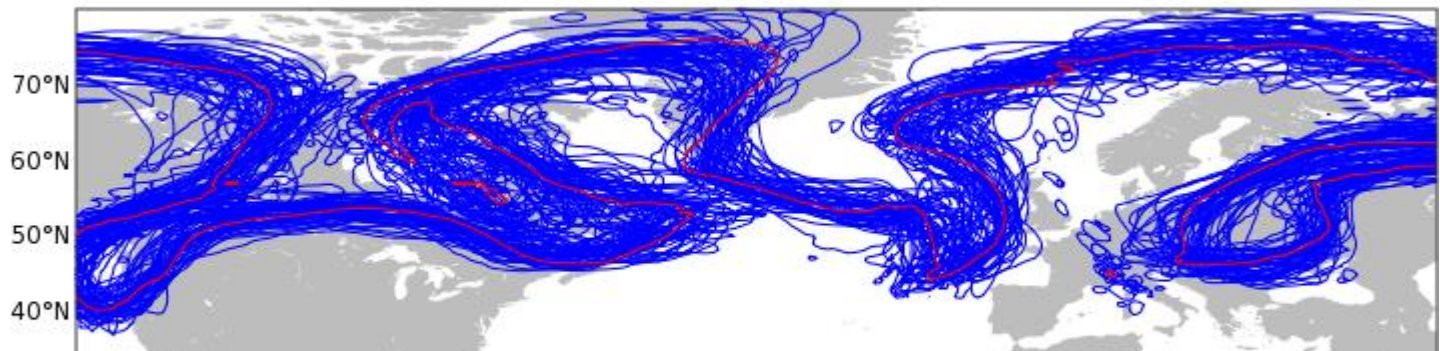
- Monitoring of evolution in **hres** and confirmation with **ensemble**

Maxi Böttcher and Julian Quinting

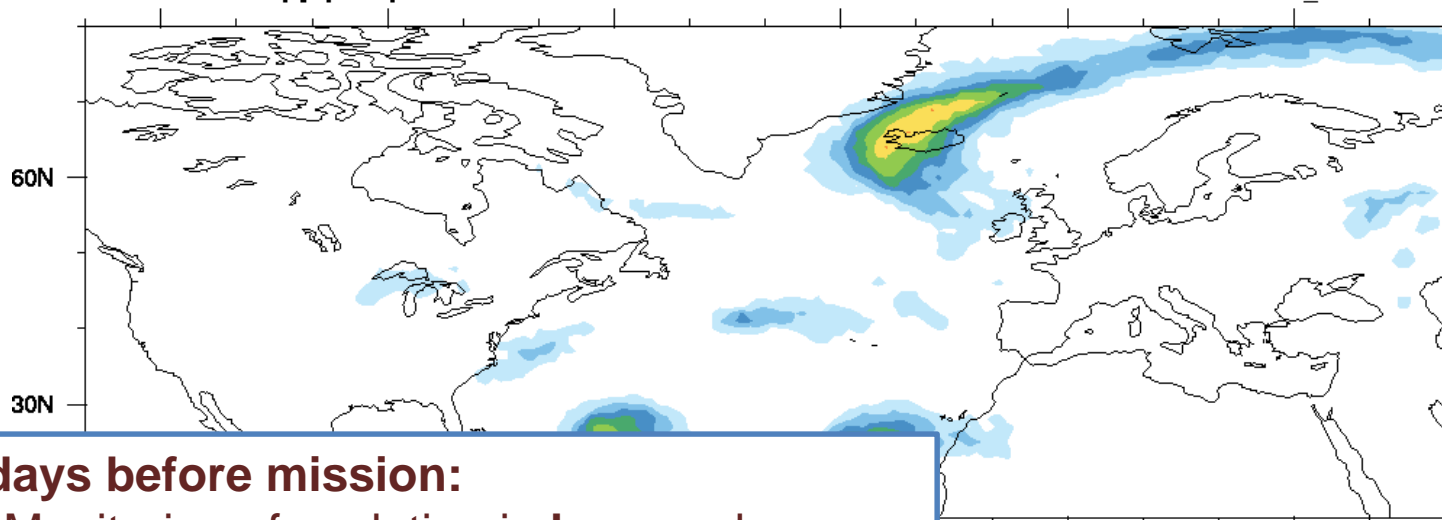
ECMWF ENSEMBLE FC

BT: 20160918 00UTC, VT: 20160921 18UTC

blue: perturbed, red: control



10400hPa: Probability [%] of traj. occurrence in ENS



3 days before mission:

- Monitoring of evolution in **hres** and confirmation with **ensemble**

10 20 30 40 50 60 70 80 90

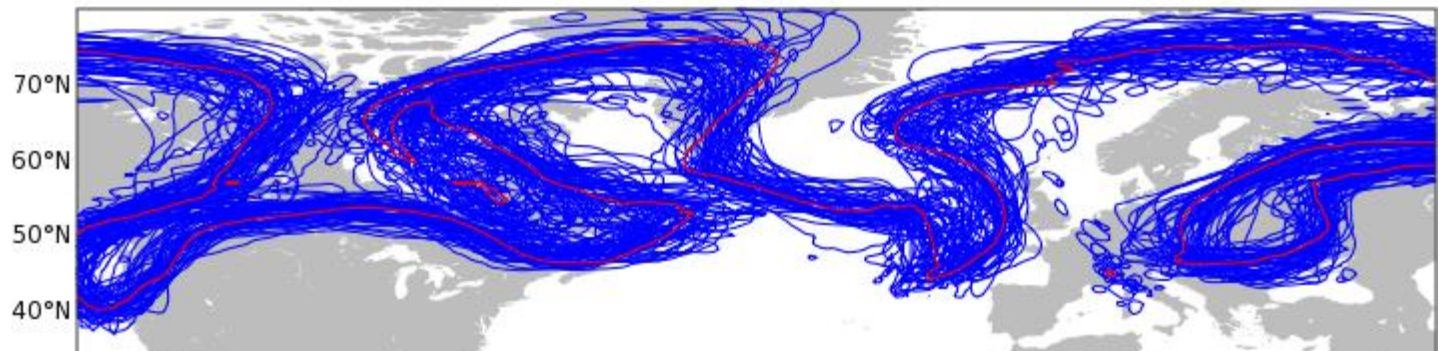
Forecast for Wed, 21 Sep 2016 18 UTC – Model consistency

BT18/00Z

ECMWF ENSEMBLE FC

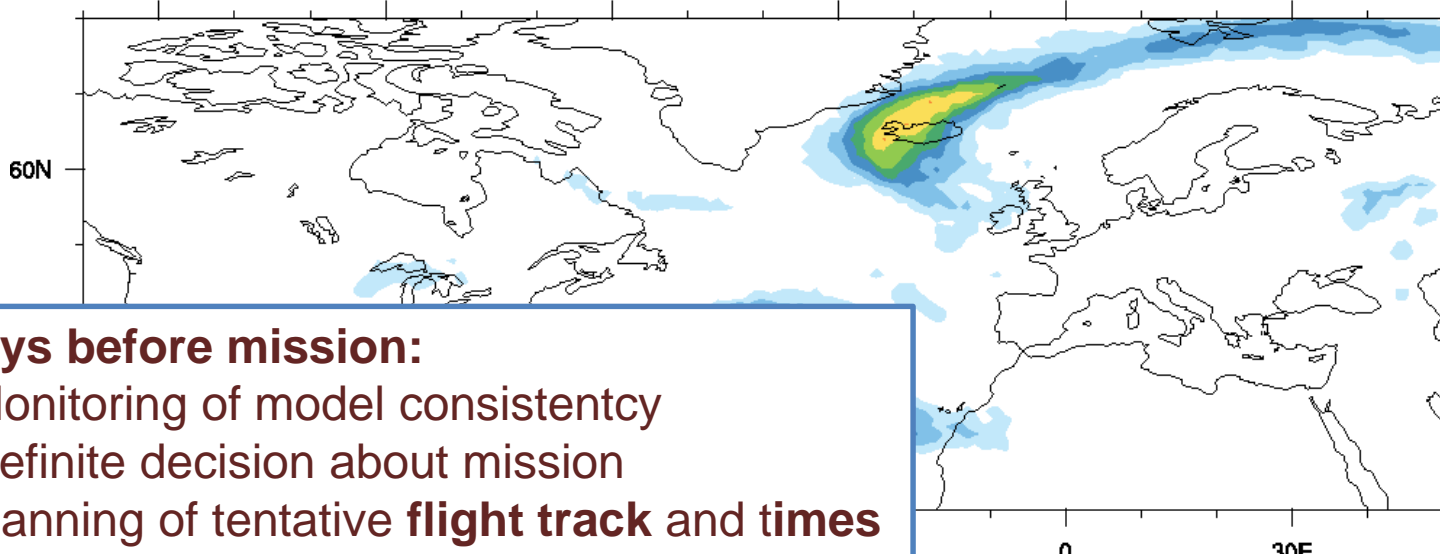
BT: 20160918 00UTC, VT: 20160921 18UTC

blue: perturbed, red: control



ECMWF ensemble forecast
BT 20160918_00UTC
VT 20160921_18UTC

1000hPa: Probability [%] of traj. occurrence in ENS



2 days before mission:

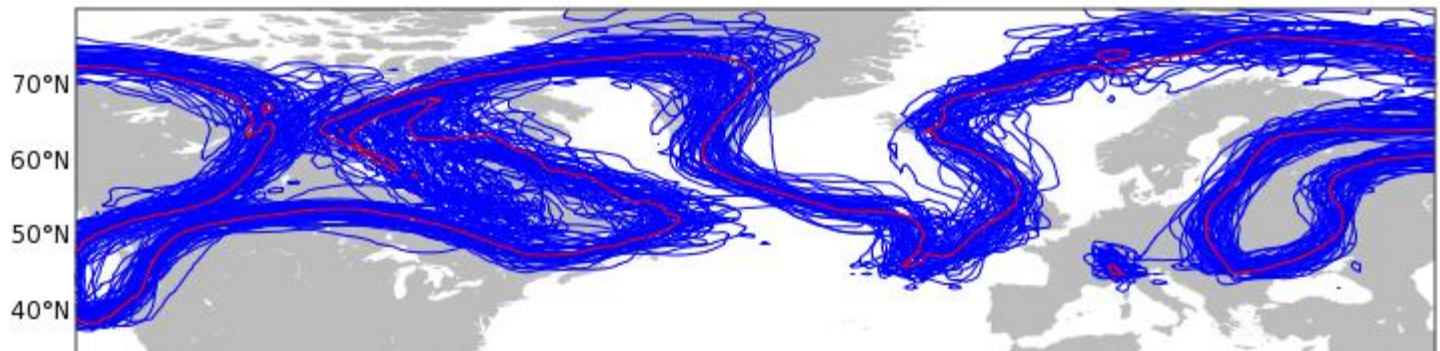
- Monitoring of model consistency
- Definite decision about mission
- planning of tentative **flight track and times**



Forecast for Wed, 21 Sep 2016 18 UTC – Model consistency

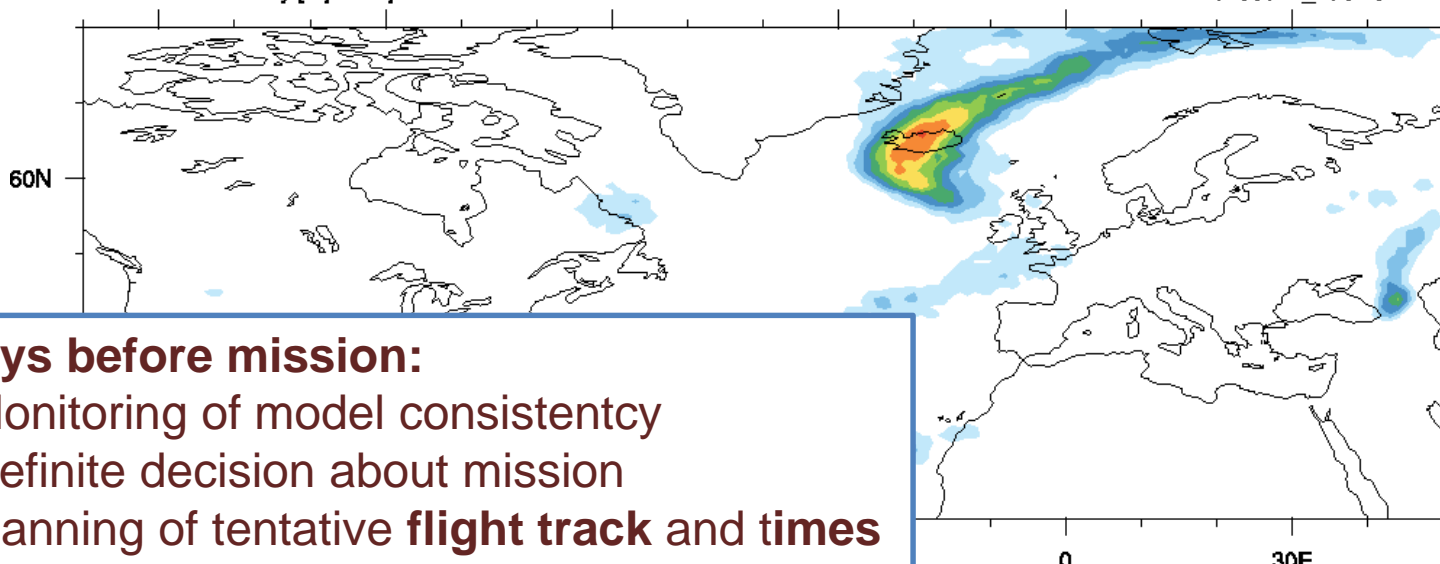
BT18/122

ECMWF ENSEMBLE FC
BT: 20160918 12UTC, VT: 20160921 18UTC
blue: perturbed, red: control



lt400hPa: Probability [%] of traj. occurrence in ENS

ECMWF ensemble forecast
BT 20160918_12UTC
VT 20160921_18UTC



2 days before mission:

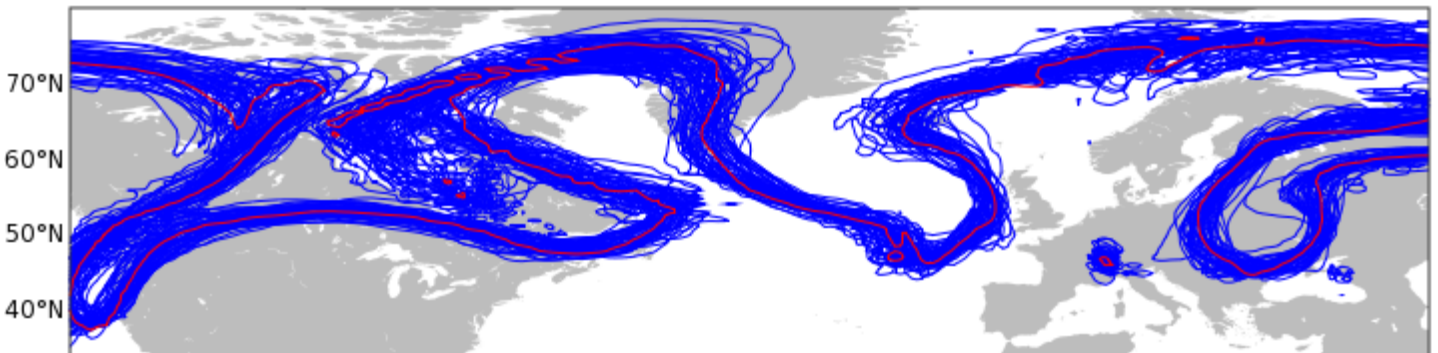
- Monitoring of model consistency
- Definite decision about mission
- planning of tentative **flight track and times**



Forecast for Wed, 21 Sep 2016 18 UTC – Model consistency

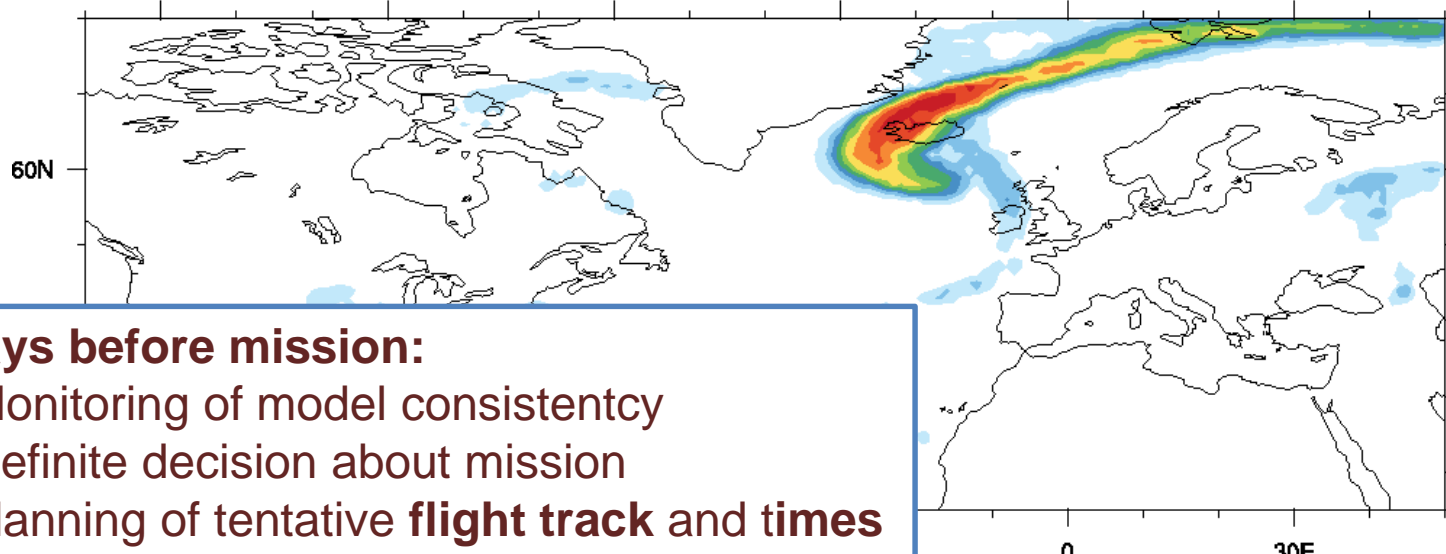
BT19/00Z

ECMWF ENSEMBLE FC
BT: 20160919 00UTC, VT: 20160921 18UTC
blue: perturbed, red: control



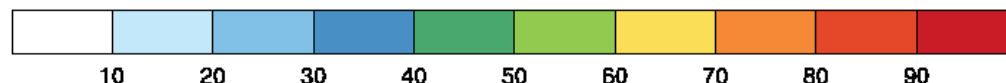
10400hPa: Probability [%] of traj. occurrence in ENS

ECMWF ensemble forecast
BT 20160919_00UTC
VT 20160921_18UTC



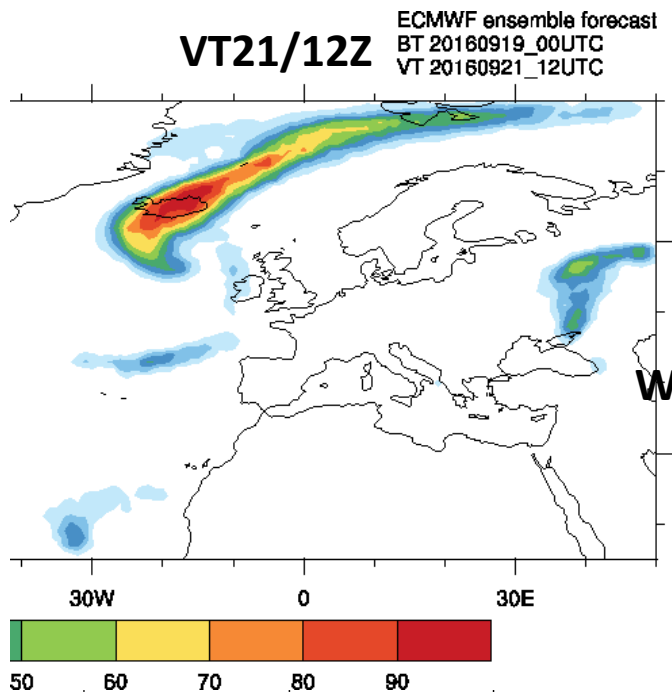
2 days before mission:

- Monitoring of model consistency
- Definite decision about mission
- planning of tentative **flight track and times**

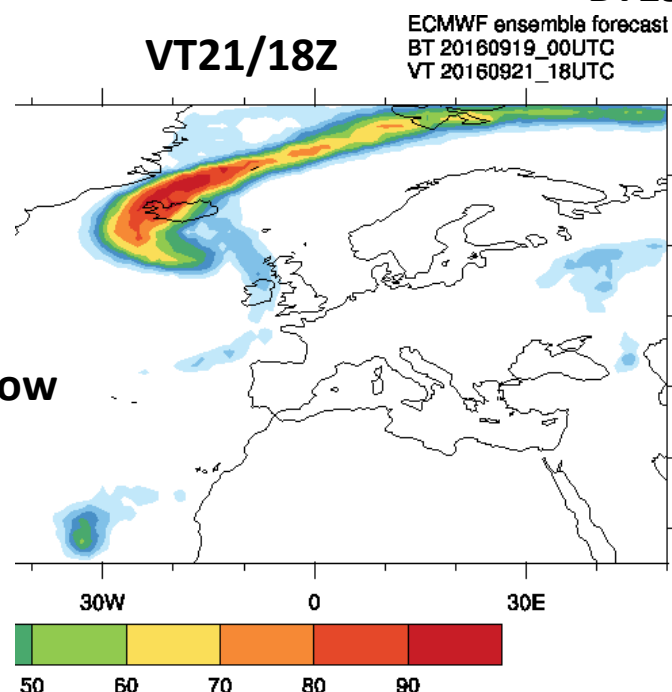


Forecast for Wed, 21 Sep 2016 18 UTC – Model consistency

BT19/00Z



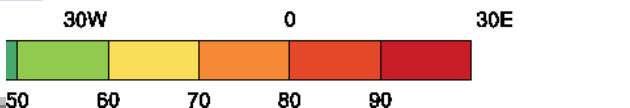
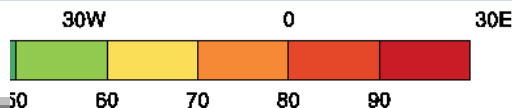
WCB outflow



WCB ascent

2 days before mission:

- Monitoring of model consistency
- Definite decision about mission
- planning of tentative **flight track and times**

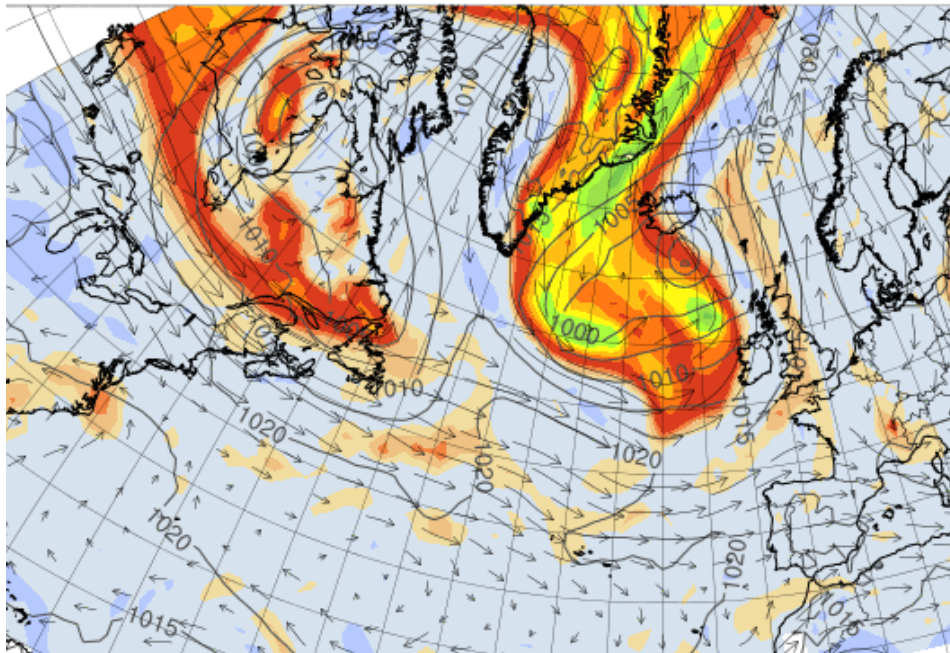


Mission on Wednesday 21 Sep 2016 15 UTC

WCB probabilités 21/12UTC

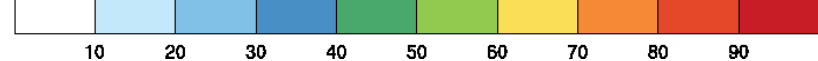
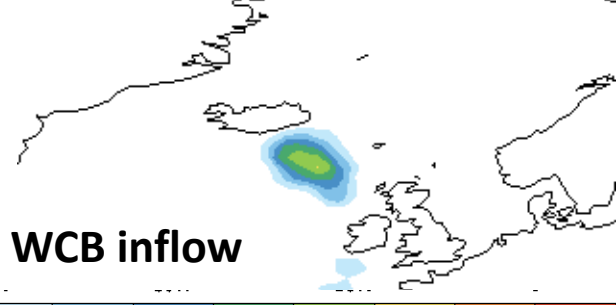
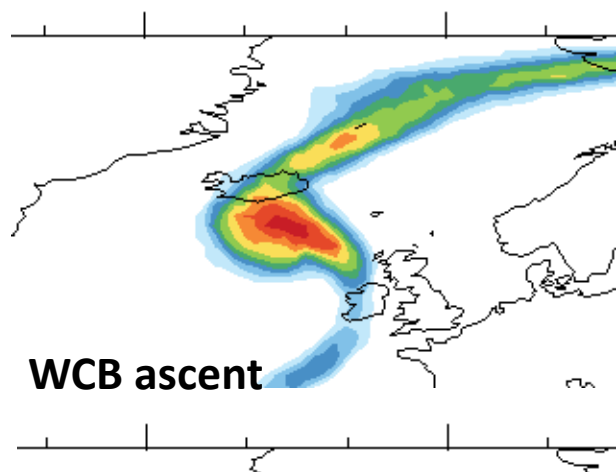
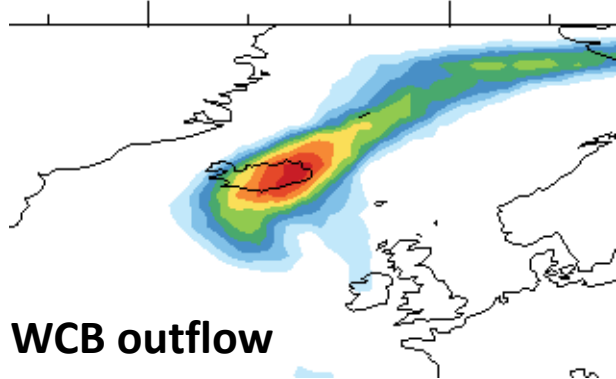
BT19/12Z

PV@315K at 20160921_15



1 days before mission:

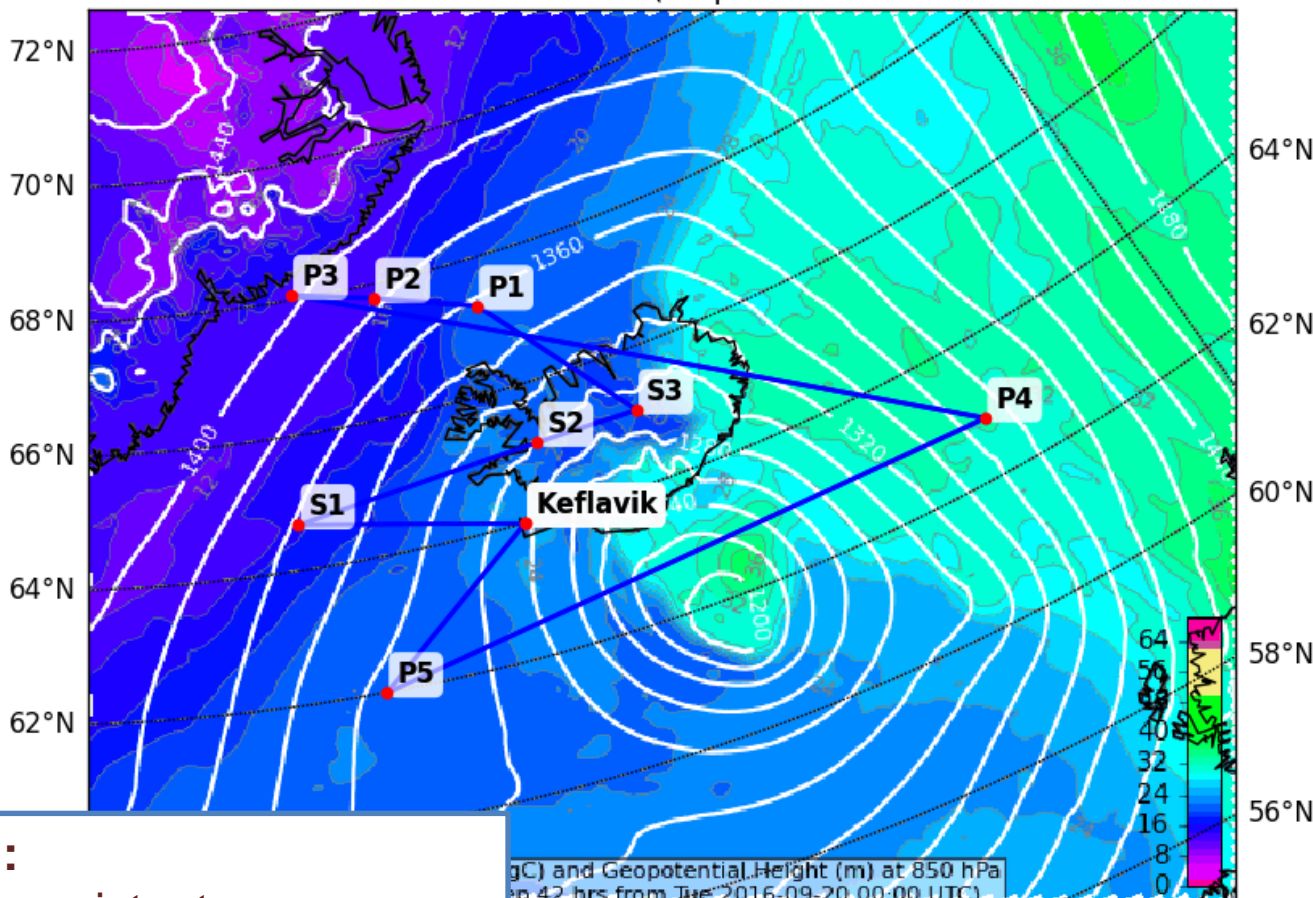
- Monitoring of model consistency
- Finalisation of flight track:
 - Location & times
 - levels



Flight pattern for Wednesday 21 September, 18UTC

HALO

Equivalent Potential Temperature (degC) and Geopotential Height (m) at 850 hPa
Valid: Wed 2016-09-21 18:00 UTC (step 42 hrs from Tue 2016-09-20 00:00 UTC)



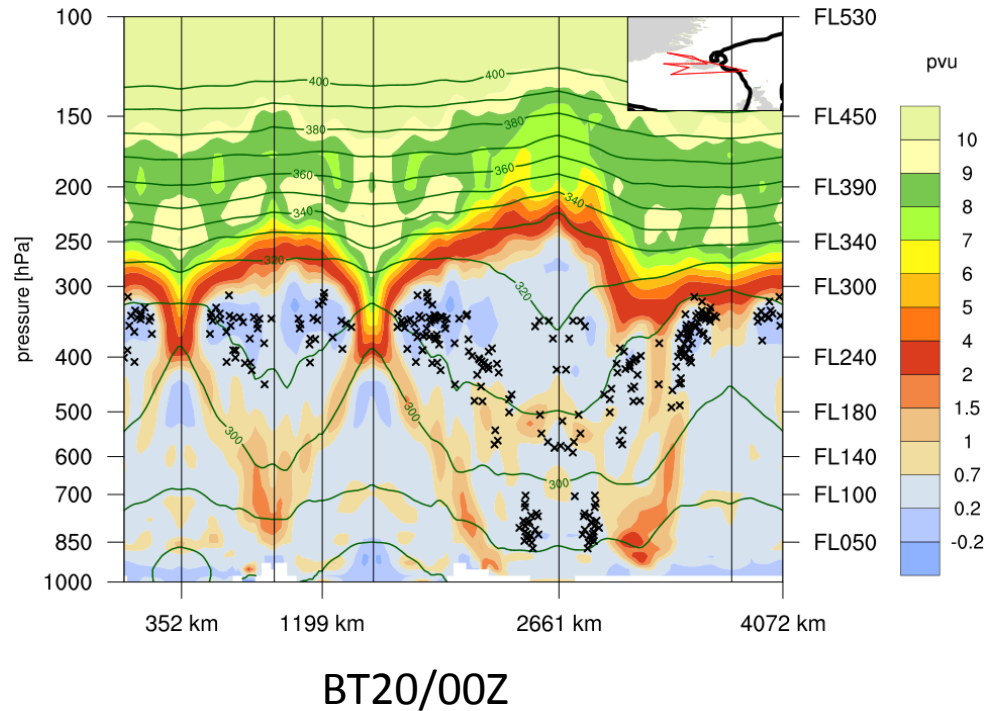
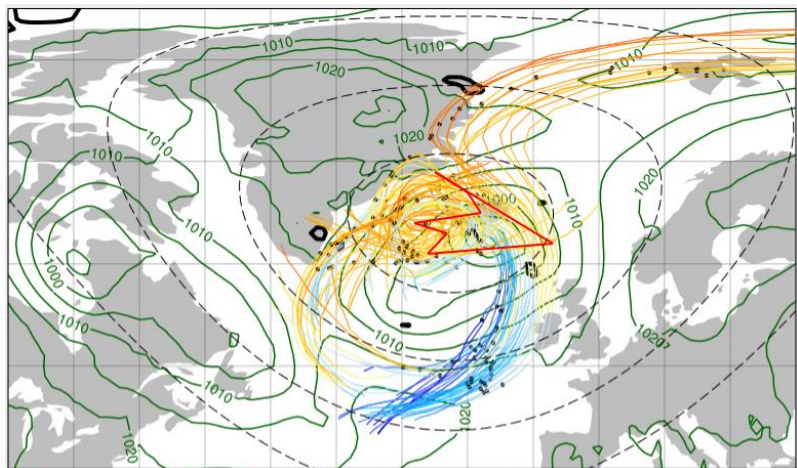
1 days before mission:

- Monitoring of model consistency
- Finalisation of flight track:
 - **Location & times**
 - **levels**

Sampling TP structure
region / warm sector 8 sondes

Trajectories from HALO flight track VT 21/18Z

HALO



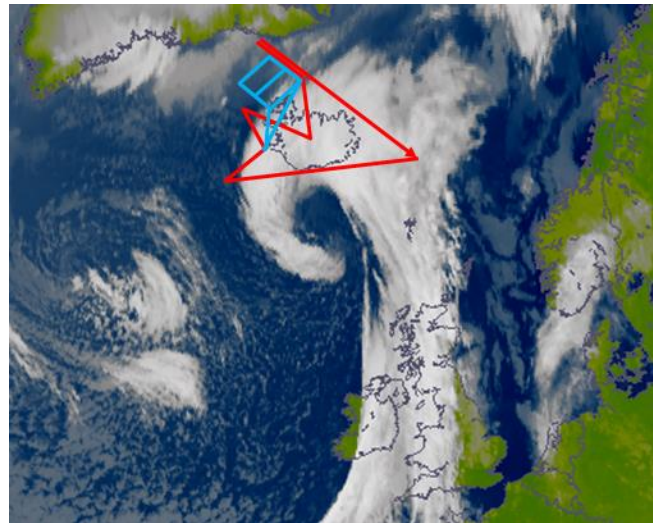
BT20/00Z

1 days before mission:

- Monitoring of model consistency
- Finalisation of flight track:
 - **Location & times**
 - **levels**

Maxi Böttcher and Julian Quinting

Successful Mission!

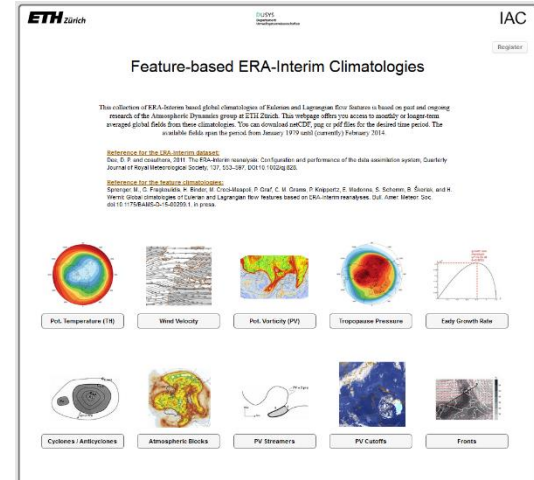
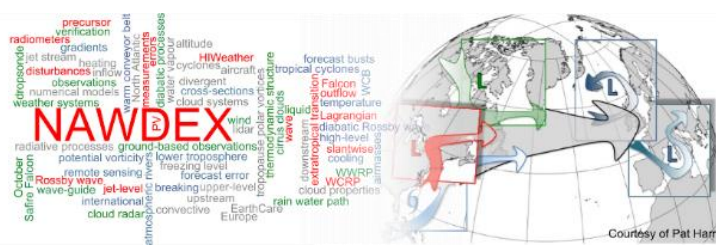
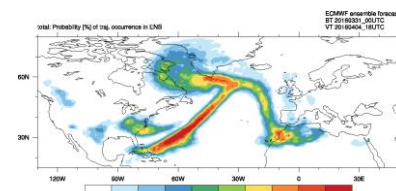
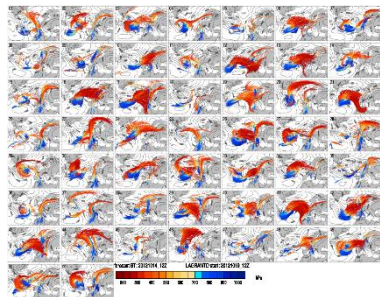


6. Summary and Outlook

- Comprehensive catalogue of feature-based ERA-I climatologies
<http://eraiclim.ethz.ch/>

- LAGRANTO trajectory model
<http://lagranto.ethz.ch/>

→ facilitate research of atmospheric dynamics from a weather system perspective



- Specific forecast products enable flight planning for atmospheric measurement campaigns
<http://nawdex.ethz.ch/>

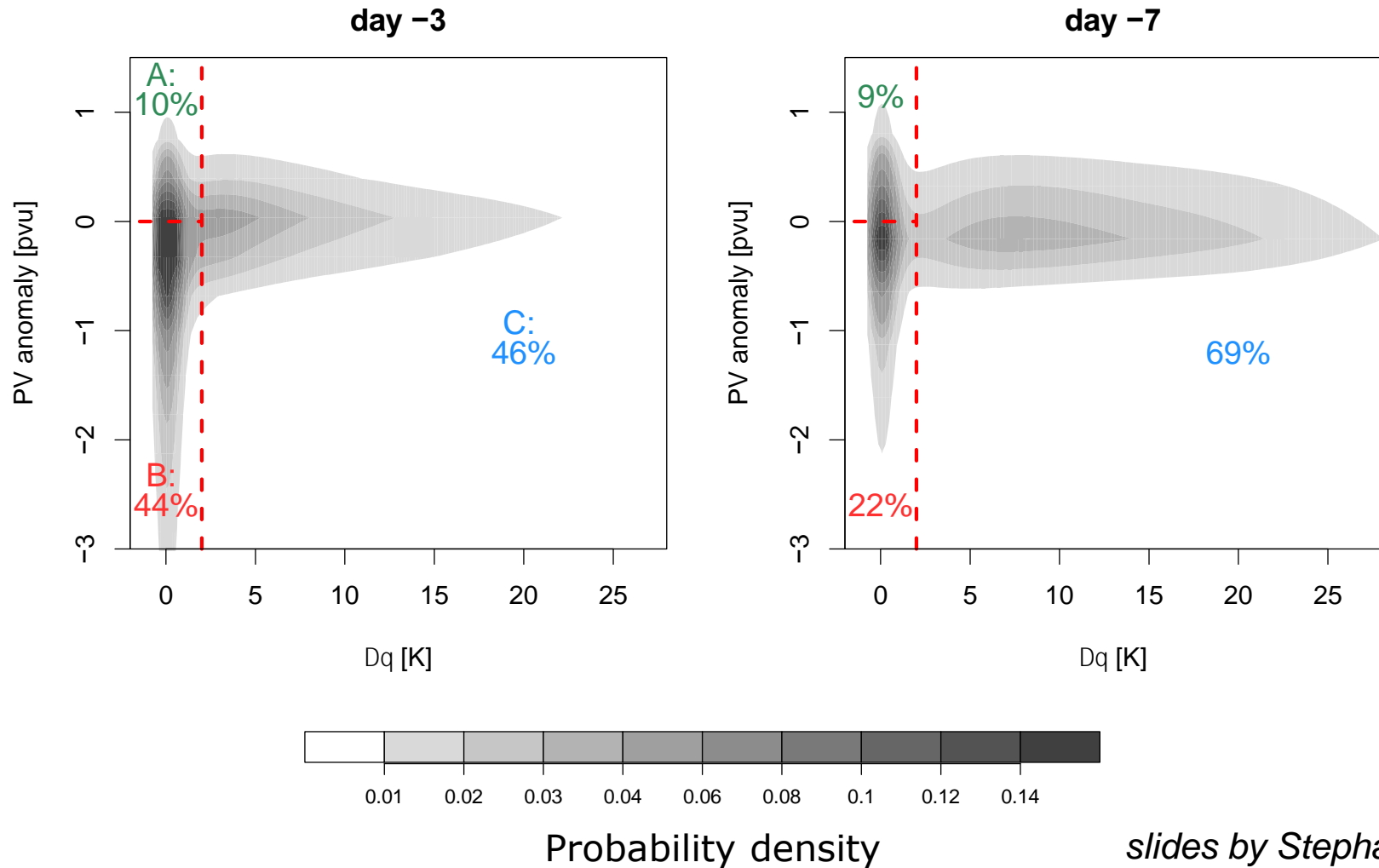
ERA-5 !?

A. Diabatic influences on blocking

Pfahl, S., C. Schwierz, M. Croci-Maspoli, C. M. Grams, and H. Wernli, 2015: Importance of latent heat release in ascending air streams for atmospheric blocking. *Nature Geosci*, **8**, 610–614, [doi:10.1038/ngeo2487](https://doi.org/10.1038/ngeo2487).

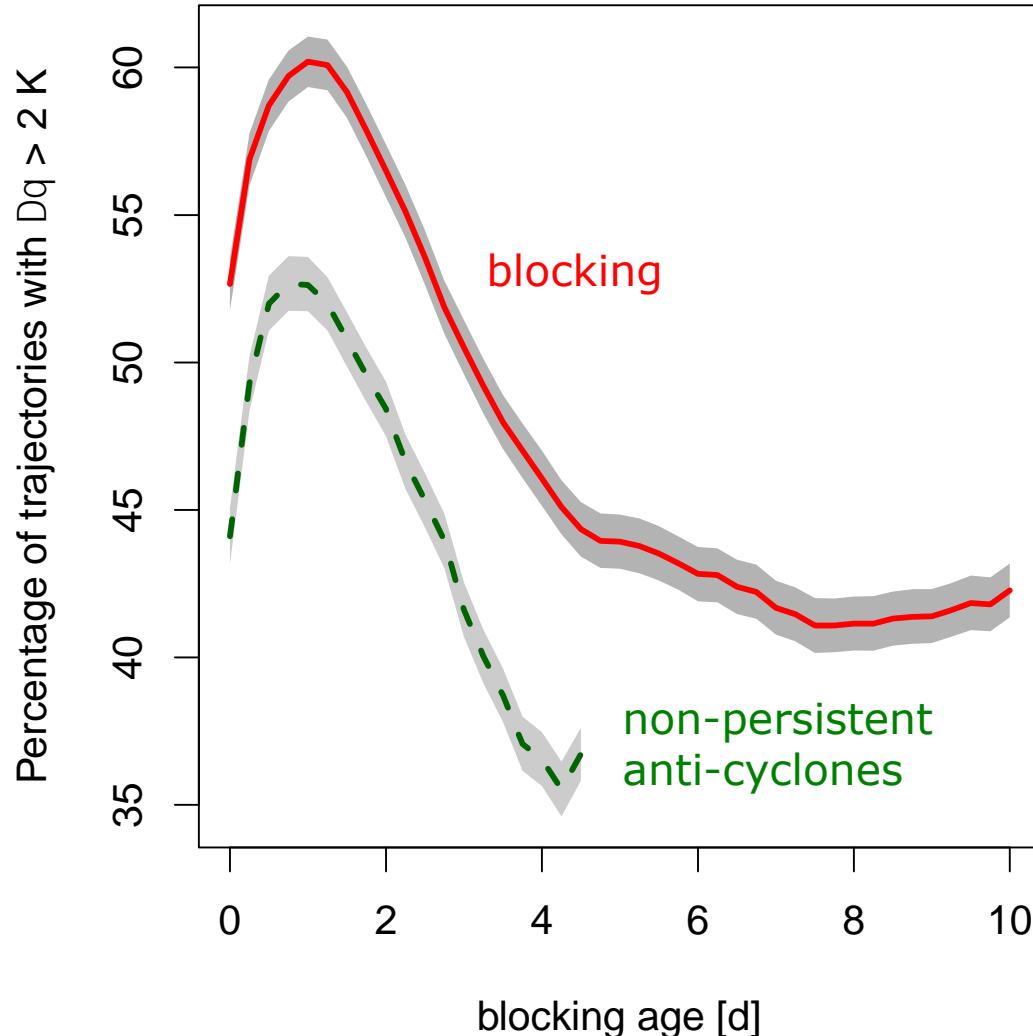
Diabatic heating and PV anomalies

Pfahl, S., et al. (2015), *NatGeo*, doi:10.1038/ngeo2487.



Diabatic heating during blocking life cycle

Pfahl, S., et al. (2015), *NatGeo*, doi:10.1038/ngeo2487.

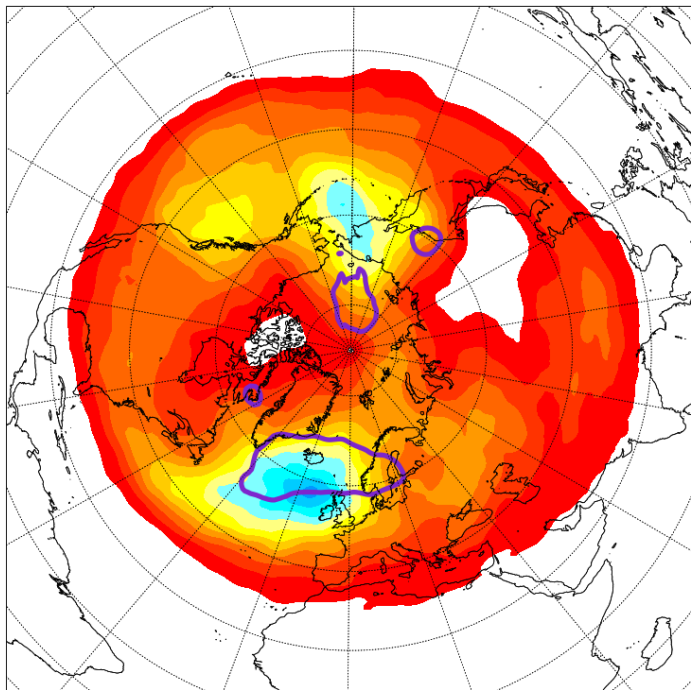


slides by Stephan Pfahl

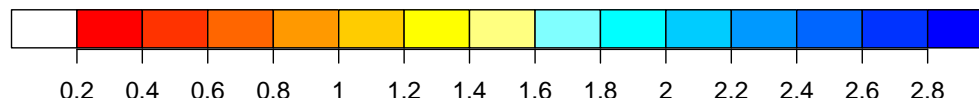
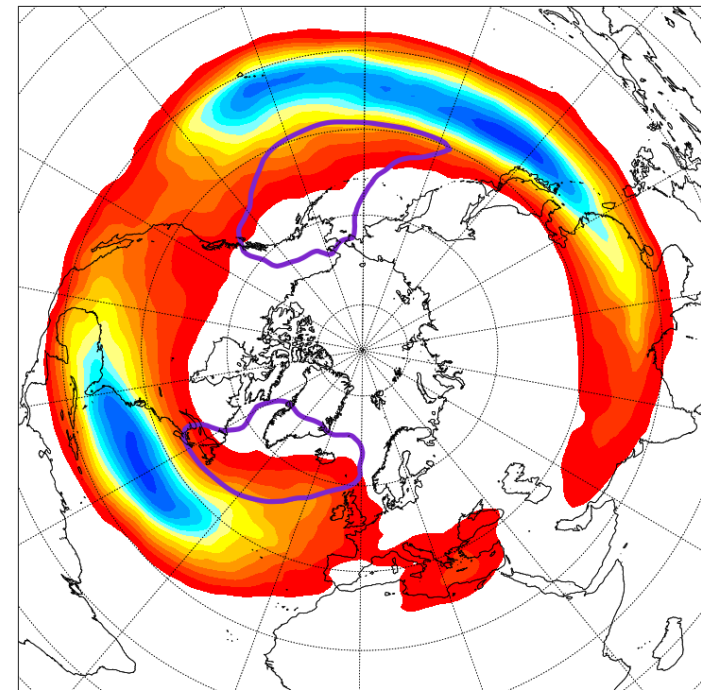
Spatial distributions of trajectories

Pfahl, S., et al. (2015), *NatGeo*, doi:10.1038/ngeo2487.

Adiabatic trajectories (cat. B)



Diabatic trajectories (cat. C)



Normalized trajectory density 3 days before arrival in the blocking region for winter. Purple contour indicates main trajectory starting regions.

slides by Stephan Pfahl

A. Potential Vorticity

Potential vorticity

$$PV = \frac{1}{\rho} \vec{\eta} \cdot \nabla \Theta$$

$$PV = \frac{1}{\rho} \eta \frac{\partial \Theta}{\partial z}$$

unit: 1PVU = $10^{-6} \text{ K m}^2 \text{ kg}^{-1} \text{ s}^{-1}$

$\eta = f + \vec{k} \cdot \nabla \times \vec{v}_h$ Absolute vorticity /
horizontal flow

Vertical stratification of
the atmosphere/stability

$$\frac{dPV}{dt} = \frac{1}{\rho} \vec{\eta} \cdot \nabla \dot{\Theta} + \frac{1}{\rho} (\nabla \times \vec{F}) \cdot \nabla \Theta$$

Total change
in PV

diabatic PV
modification

frictional
processes

- PV is conserved under adiabatic frictionless flow (**conservation principle**)
 - use PV as air mass tracer on isentropic surfaces to identify PV signatures of weather systems
- PV can be inverted given a balance condition and boundary conditions (**inversion principle**)
 - derive wind, T, p field from a given PV distribution

Potential vorticity

$$PV = \frac{1}{\rho} \vec{\eta} \cdot \nabla \Theta$$

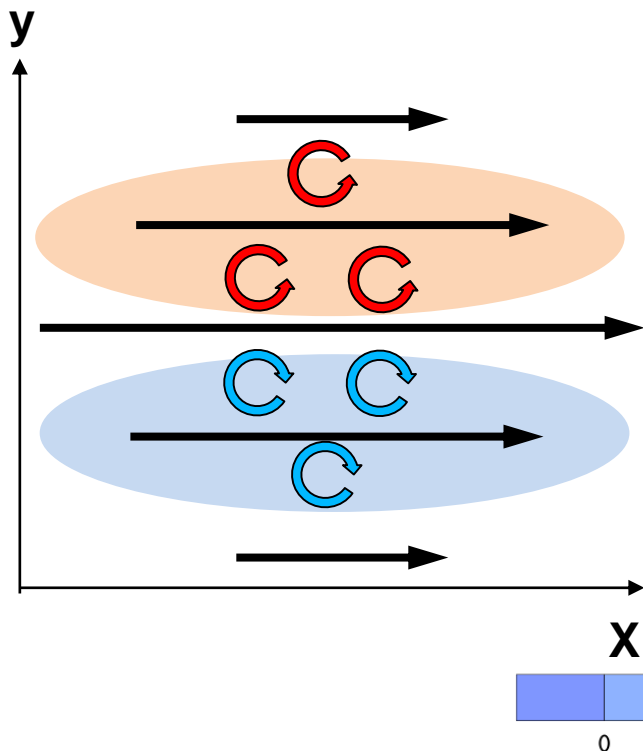
$$PV = \frac{1}{\rho} \eta \frac{\partial \Theta}{\partial z}$$

unit: $1\text{PVU} = 10^{-6} \text{ K m}^2 \text{ kg}^{-1} \text{ s}^{-1}$

$$\eta = f + \vec{k} \cdot \nabla \times \vec{v}_h$$

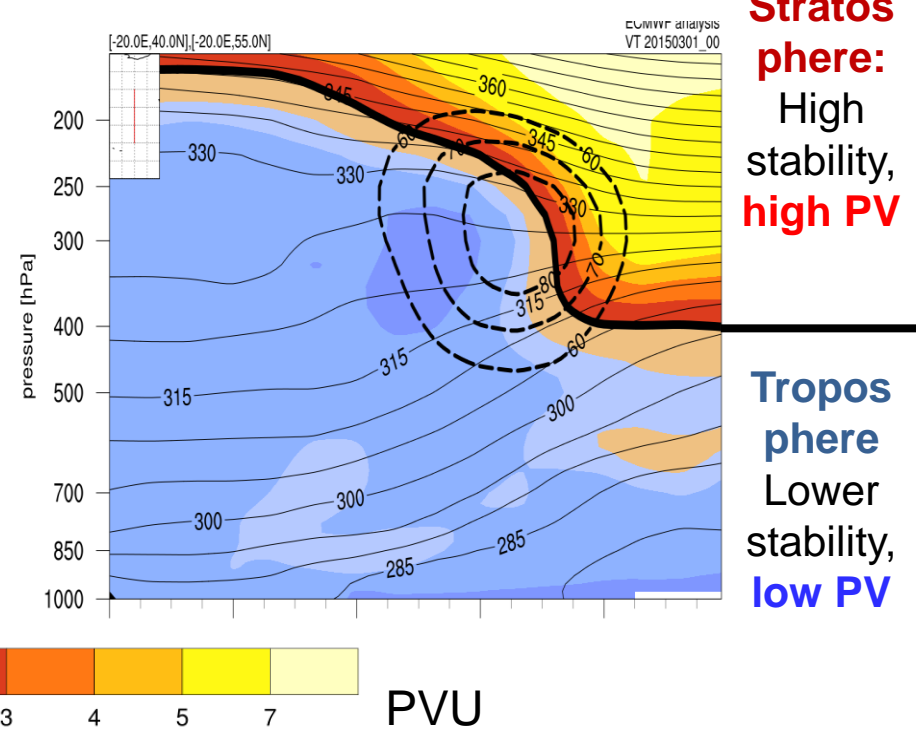
Absolute vorticity / horizontal flow

Vertical stratification of the atmosphere/stability



North of jet streak
Pos. shear vorticity,
high PV

South of jet streak
neg. shear vorticity,
low PV



Stratosphere:
High stability,
high PV

Troposphere
Lower stability,
low PV